Flamingo participates in multiple models of cell competition

Pablo Sanchez Bosch[1,2], Bomsoo Cho[1,2], Jeffrey D. Axelrod[1*]

1. Department of Pathology, Stanford University School of Medicine, 300 Pasteur Dr., Stanford CA, 94305, USA
2. These authors made equal contributions.

* Corresponding author

Abstract

The growth and survival of cells with different fitness, such as those with a proliferative advantage or a deleterious mutation, is controlled through cell competition. During development, cell competition enables healthy cells to eliminate less fit cells that could jeopardize tissue integrity, and facilitates the elimination of pre-malignant cells by healthy cells as a surveillance mechanism to prevent oncogenesis. Malignant cells also benefit from cell competition to promote their expansion. Despite its ubiquitous presence, the mechanisms governing cell competition, particularly those common to developmental competition and tumorigenesis, are poorly understood. Here, we show that in *Drosophila*, the planar cell polarity (PCP) protein Flamingo (Fmi) is required by winners to maintain their status during cell competition in malignant tumors to overtake healthy tissue, in pre-malignant cells as they grow among wildtype cells, in healthy cells to eliminate pre-malignant cells, and by supercompetitors to occupy excessive territory within wildtype tissues. "Would-be" winners that lack Fmi are unable to over-proliferate, and instead become losers. We demonstrate that the role of Fmi in cell competition is independent of PCP, and that it uses a distinct mechanism that may more closely resemble one used in other less well defined functions of Fmi.

Introduction

Dividing cells in proliferative tissues must maintain tissue homeostasis and structural integrity as well as preserve their genetic integrity. One of the mechanisms operating in proliferative tissues to achieve these requirements is cell competition. Cell competition is a process in which cells of a higher fitness ("winners") eliminate less fit neighbors ("losers"), by inducing either cell death (Norman *et al.*, 2012; Meyer *et al.*, 2014; Di Giacomo *et al.*, 2017; Watanabe *et al.*, 2018) or extrusion from the epithelial layer (Norman *et al.*, 2012; Kon *et al.*, 2017; Kohashi *et al.*, 2021). Cell competition was first recognized in 1975(Morata and Ripoll, 1975) , when Morata and Ripoll studied the growth of Drosophila carrying a mutation in the gene for the ribosomal protein RpS17 (termed *minute*). Animals heterozygous for this

minute mutation are viable but develop slowly due to decreased proliferation rates. They further observed that clones of cells carrying this *minute* mutation in a wildtype background were actively eliminated from the *Drosophila* developing wing. Since then, extensive advances have been made in our understanding of the process (reviewed in (Morata, 2021)). We now know that cell competition can be triggered by mutations that cause a disadvantage, such as the aforementioned *minute* cells, and can also be triggered by mutations that confer a proliferative advantage, such as ectopic expression of proto-oncogenes such as Myc or Ras (de la Cova *et al.*, 2004; Moreno and Basler, 2004; Hogan *et al.*, 2009). In this case, the process is known as super-competition, and WT cells behave as losers and are eliminated from the tissue by the mutant super-competitors. The "survival of the fittest" effect observed in cell competition has been shown to be critical during embryonic and larval development as well as for tissue homeostasis (Amoyel and Bach, 2014; Maruyama and Fujita, 2017; Morata, 2021). Much additional research has shown that cells and their neighbors are constantly evaluating their fitness, and that the active elimination of less fit cells is critical to maintain tissue integrity (Ellis *et al.*, 2019), maintain chromosomal stability (Baillon *et al.*, 2018; Ji *et al.*, 2021), ameliorate effects of cellular aging (Merino *et al.*, 2015) and suppress tumorigenesis (Kon *et al.*, 2017; de Vreede *et al.*, 2022).

While cell competition has been observed in many cell types, much attention has focused on studies in epithelia (Vincent *et al.*, 2013). Polarity is a hallmark of epithelial tissues, and loss of polarity plays a prominent role in triggering cell competition and in the process of eliminating loser cells. Cells harboring mutations in apicobasal polarity genes have been shown to induce and/or regulate cell competition when surrounded by WT cells. In *Drosophila*, mutations in apicobasal polarity genes *scribble* (*scrib*), *discs large* (*dlg*), and *lethal giant larva* (*lgl*) all trigger cell competition when induced clonally (i.e. surrounded by WT cells), and the clones are eliminated from the epithelial tissue (Hariharan and Bilder, 2006; Morata and Calleja, 2020). However, clones that are deficient for any of these polarity genes can survive if they are competing against less fit cells, or if they carry additional mutations that confer a growth advantage. For example, when *lgl* clones, which would be eliminated when surrounded by WT cells, are made to express elevated levels of Myc, the competition is reversed, and they instead become winners (Froldi *et al.*, 2010). This context-dependence and fitness surveillance highlights the complexity of cell competition and its plasticity.

In epithelial tissues, cell competition is critical to suppress tumorigenesis, as polarity-deficient clones are prone to malignancy. When *scrib* mutant epithelial cells acquire elevated activity of a proto-oncogene such as the constitutively active Ras^{V12}, these clones acquire malignant properties of ectopic growth and invasiveness (Brumby and Richardson, 2003; Pagliarini and Xu, 2003). Surveillance and rapid elimination of cells that develop polarity defects therefore serves to protect epithelia from oncogenesis. This competitive mechanism is known as Epithelial Defense Against Cancer, or EDAC (Maruyama and Fujita, 2017; Kon and Fujita, 2021). Through EDAC, normal epithelial cells eliminate neighboring transformed cells by inducing apoptosis or by inducing their apical or basal extrusion from the epithelial layer (Watanabe *et al.*, 2018; Kohashi *et al.*, 2021) . On the other hand, tumors that exhibit more aggressive properties and escape the defense mechanisms not only proliferate but actively engage in cell competition to promote their own growth and malignancy (Vishwakarma and Piddini, 2020; Madan *et al.*, 2022). For example, growth of *Drosophila* $APC^{-/-}$ intestinal adenomas requires active elimination of WT cells, and inhibiting cell death in the WT tissue hampers adenoma growth (Suijkerbuijk *et al.*, 2016).

In addition to apicobasal polarity, epithelial tissues are planar polarized. Planar cell polarity (PCP) signaling polarizes cells within the plane of the epithelium to orient cellular structures, cell divisions, and

cell migration during development and homeostasis (Adler, 2002; Simons and Mlodzik, 2008; Vladar *et al.*, 2009; Butler and Wallingford, 2017). Intercellular Fmi homodimers scaffold the assembly of a set of core PCP proteins: on one side of a cell, Frizzled (Fz), Dishevelled (Dsh), and Diego (Dgo) comprise a complex that interacts with another complex containing Van Gogh (Vang) and Prickle (Pk) on the opposite side of the adjacent cell. Fmi homodimers transmit differential signals in opposite directions to communicate the presence of either protein complex to the other, linking the proximal and distal complexes and mediating asymmetric signaling between them (Lawrence *et al.*, 2004; Strutt and Strutt, 2007; Chen *et al.*, 2008; Strutt and Strutt, 2008; Struhl *et al.*, 2012). In addition to establishing planar polarity, numerous reports have suggested links between PCP signaling and cancer progression, promoting cell motility, invasiveness and metastasis (Weeraratna *et al.*, 2002; Katoh, 2005; Katoh and Katoh, 2007; Coyle *et al.*, 2008; Gujral *et al.*, 2014; VanderVorst *et al.*, 2018, 2023). Its roles, however, remain poorly characterized.

To probe a potential connection between PCP and cancer, we employed a *Drosophila* eye tumor model. We discovered a requirement for Fmi, but not other core PCP proteins, in tumor associated cell competition. We found that aggressive tumors require Fmi to outcompete the neighboring WT tissue. We then found that this Fmi requirement is not unique to tumor competition; in several developmental cell competition scenarios, removing Fmi from winner cells prevents them from eliminating their neighbors and transforms them into losers. “Would be” winners that lack Fmi show both a decrease in proliferation and an increase in apoptosis. By several criteria, we show that this function for Fmi is independent of its role in PCP signaling.

Results

Flamingo is required for tumorigenesis in Drosophila Ras^{V12} tumors

Planar polarity has been linked to tumorigenesis in several organisms, tumor models, and patient samples (Kaucká *et al.*, 2013; Asad *et al.*, 2014; Puvirajesinghe *et al.*, 2016; VanderVorst *et al.*, 2018; Chen *et al.*, 2021b, 2021c; Li *et al.*, 2021). We explored how the core PCP complex might be involved in tumorigenesis. To do so, we used the versatile and widely used Ras^{V12} tumor model in Drosophila eye imaginal discs. In this model, eye disc cells are transformed into highly tumorigenic cells by co-expressing the constitutively active Ras^{V12} oncoprotein and RNAi against the tumor suppressor Scribble (Scrib) (Pagliarini and Xu, 2003). Cells expressing these genes quickly expand into massive tumors and invade the neighboring brain tissue (Fig 1A-C).

To study the requirement for PCP signaling in tumors, we expressed Ras^{v12} and *scrib* RNAi throughout the eye, and simultaneously down-regulated PCP core proteins by also expressing validated RNAi’s against *fmi*, *fz*, *dsh*, *vang*, and *pk*. We then imaged tumor size through the pupal cuticle. We observed that tumor growth was unaffected by knockdown of any of the core PCP genes (Fig 1A-H). We then asked whether PCP signaling might be required by tumors when they’re confronted by WT cells. To test this hypothesis, we created clonal tumors in the eye disc by expressing *Ras^{V12}* and *scrib* RNAi under control of ey-Flp. In this model, nearly every cell in the eye disc will perform chromosomal recombination, producing an eye disc composed of approximately 50% WT and 50% tumor cells. Under these conditions, tumor cells expand aggressively, displacing WT cells and causing massive overgrowth of the eye disc and metastasis to the larval brain (Fig 1I-K). We created clonal tumors that were also null

for either *fmi*, *fz*, *dgo*, *vang*, or *pk* and evaluated them for their ability to grow and metastasize when confronted with wildtype cells (Fig 1I-P). Remarkably, only *fmi* interfered with tumorigenesis, restraining growth of tumors in the eye disc and preventing them from invading neighboring tissues (Fig 1L). Because this effect was only apparent when tumors were induced in juxtaposition to wildtype cells, we hypothesized that Fmi may only be required in tumors that undergo cell competition.

Flamingo is required in winner cells during cell competition

The molecular mechanisms of tumor competition and developmental cell competition are highly conserved and are shared by multiple processes. Mechanisms used by tumors in cell competition are sometimes shared by developmental cell competition. Just as tumors promote extrusion of surrounding wild type cells by reorganizing their cytoskeletons (Rachagani *et al.*, 2011; Shao *et al.*, 2014; Nieto *et al.*, 2016), WT cells undergo cytoskeletal reorganization to eliminate malignant cells from epithelia during EDAC (Maruyama and Fujita, 2017). Induction of JNK-mediated cell death is also common to developmental competition and tumor cell competition, as shown in intestinal adenomas (Suijkerbuijk *et al.*, 2016). We hypothesized that the requirement of Fmi by competing tumors might also be shared in developmental cell competition. We therefore evaluated the role of Fmi in non-malignant, developmental cell competition models.

Cells expressing high levels of Myc behave as winners when growing among wildtype cells, proliferating faster than wildtype cells and inducing their elimination. Despite Myc being a proto-oncogene, in contrast to Ras^{v12} *scrib* RNAi tumors, Myc overexpressing clones do not become tumors, but instead expand to occupy larger than normal domains of morphologically normal tissue (de la Cova *et al.*, 2004; Moreno and Basler, 2004; Clavería *et al.*, 2013). As for the Ras^{v12} *scrib* RNAi tumor model, we used UAS-myc and ey-Flp to create eye discs comprising initially equal populations of Myc overexpressing (>>Myc) and wildtype cells. As expected, >>Myc cells outcompeted WT cells, and the majority of cells (~65%) in late third instar discs were >>Myc cells (Fig 2A). However, when >>Myc cells were depleted of *fmi*, they failed to outcompete WT cells and instead became losers. Wildtype cells outcompeted >>Myc, $fmi^{-/-}$ cells such that late third instar eye discs were composed of only ~35% >>Myc cells, indicating that they not only failed to behave as winners, but are outcompeted by the wildtype cells (Fig 2B-C).

If the requirement of Fmi is a general feature of cell competition, it should be observable in other tissues. We therefore assessed whether depleting Fmi in wing disc >>Myc winner clones would also reverse the competition outcome. We used hsp-Flp to generate twin spot clones expressing UAS-Myc, and as in eye discs, those clones outcompeted neighboring WT cells. Myc supercompetitors clones were on average 1.7 times larger than the RFP+ twin spots (Fig 2D). However, when >>Myc clones lacked Fmi, their ability to compete was severely impaired, producing much smaller clones, being on average half as large as their RFP+ twin spots, and thus, like in eye discs, becoming losers when competing against wildtype cells (Fig. 2-E-F). $fmi^{-/-}$ Myc clones were also highly fragmented. Importantly, making cells mutant for *fmi* alone had no effect on their growth in either the eye or wing disc (Supp fig 1).

In the setting of tumorigenesis, either tumor cells or wildtype cells may emerge as winners of cell competition. Tumors outcompete wildtype cells in the processes of invasion and metastasis, whereas transformed pre-malignant cells are often eliminated by wildtype cells through competition-dependent defense mechanisms such as EDAC (Kon *et al.*, 2017; Kon and Fujita, 2021). We therefore further explored the potential requirement for Fmi in a system in which both outcomes occur at different times.

In eye discs, cells lacking Scribble display a proto-oncogenic behavior, losing polarity and behaving as winners, over-proliferating in the developing eye disc. However, they subsequently become losers, and are eliminated via JNK-mediated apoptosis during pupal development so that they are virtually completely absent from the tissue before the fly ecloses (Brumby and Richardson, 2003).

Using the ey-Flp system to activate RNAi against *scrib* in eye discs, we confirmed that downregulation of *scrib* induces over-proliferation in eye discs, thus causing the Scrib deficient cells to behave as winners (Fig. 2J). We then asked what was the effect of removing Fmi. As was observed for >>Myc clones, *fmi*$^{-/-}$ *scrib* RNAi clones lost their ability to win against wildtype cells and instead were actively eliminated from the eye disc by WT cells (Fig. 2K). Loss of Fmi in WT cells surrounding *scrib* RNAi clones had little effect on their growth (Fig. 2L).

We also confirmed that, later, in pupal development, *scrib* RNAi clones behave as losers and are eliminated by WT cells. The clones are completely removed before adulthood, and this loss of tissue causes the adult compound eye to be smaller compared to WT (Fig. 2I'-J' and Fig. 2I"-J"). When the *scrib* mutant cells become losers, the requirement for *fmi* is reversed. In this case, any *scrib* RNAi clones that remain after larval stage and are normally eliminated during pupal development were still eliminated if they lacked Fmi (Fig. 2K'-K"). And because most *scrib* clones were eliminated during larval development, the adult compound eye was as big as in the WT control (Fig. 2I' and K'). On the other hand, rendering the surrounding "WT" winner cells mutant for *fmi* causes them to lose their ability to eliminate *scrib* RNAi cells. The surviving *scrib* RNAi cells remained viable, but failed to differentiate, thereby producing large scars in the adult eye (Fig. 2L'-L"). We observed considerable lethality in this population of flies, presumably due to metastasis of the *scrib* RNAi cells that could not be eliminated. Thus, early, when *scrib* RNAi clones are winners, they require Fmi to win, and later, when wildtype cells become winners, the WT cells require Fmi to win.

Taken together, our results demonstrate that Fmi is required by winners in both tumorigenic and developmental cell competition models.

Loss of fmi triggers cell death and reduces proliferation in "would-be" winner clones

Our observations suggest that lack of *fmi* renders winner clones and tumors incapable of outcompeting the neighboring tissue in multiple cell competition scenarios. Cell competition relies mainly on two mechanisms to allow winner cells to take over the tissue when confronting less fit cells: faster proliferation than losers and elimination of loser cells by induced apoptosis or extrusion (Amoyel and Bach, 2014; Maruyama and Fujita, 2017; Morata, 2021). We therefore explored how the lack of *fmi* in tumors and winner >>Myc cells during competition affected both mechanisms.

Drosophila control Ras^{V12}, *scrib* RNAi eye tumors trigger apoptosis in the neighboring cells, as detected by Dcp1 staining (Fig. 3A-D), consistent with previous reports (Karim and Rubin, 1998; Pérez *et al.*, 2017) and with their highly invasive behavior when surrounded by WT cells. However, when *fmi* was removed from the clonal tumors, the outcome of this competition was reversed, as described above, and instead, *fmi*$^{-/-}$, Ras^{V12}, *scrib* RNAi tumors displayed excess apoptosis compared to the surrounding WT tissue (Fig. 3E-H). Moreover, we found cell debris from *fmi*-deficient tumor cells inside lysosomal vesicles in WT cells, suggesting that WT cells are clearing neighboring loser tumor cells through engulfment (Suppl. Fig 2). We then tested whether this reversal of apoptosis burden was specific to the tumor model, or if it is

a mechanism shared in other cell competition models. Consistent with the tumor model, eye disc >>Myc cells lacking Fmi displayed widespread apoptosis (Fig. 3I-K), likely contributing to the reversal in competition we previously observed (Fig. 2A-C).

Cell competition does not rely solely on apoptosis to eliminate loser cells. An increased proliferation rate of winners is also a hallmark of cell competition (Morata, 2021; Madan *et al.*, 2022). To evaluate whether Fmi is also required to maintain a higher proliferative ratio in winners, we quantified mitotic cells in winner clones with and without Fmi. The wing disc displays distributed cell divisions throughout larval development, in contrast to eye discs, where passing of the morphogenetic furrow limits proliferation as cells start differentiating into compound eye cells (Wolff and Ready, 1991; Tsachaki and Sprecher, 2012). Therefore, for the quantification of proliferation, the wing is a better model than the eye disc. When wing disc >>Myc clones were depleted of Fmi, cell proliferation, as measured by pHis3 staining, was significantly reduced (Fig. 3L-N). Taken together, these observations directly link the need for Fmi to proliferation and induced apoptosis, the two key events of cell competition, in several models of cell competition.

Fmi is not required for cell-cell communication between winners and losers

Cell competition is thought to rely on intercellular communication to compare fitness and determine the outcome between prospective winner and loser cells (Kon *et al.*, 2017; Baker, 2020; Ogawa *et al.*, 2021). If Fmi is involved in these determinative intercellular communication events by signaling as a trans-homodimer, it should be required in both prospective winner and loser cells. Our results examining Fmi requirement in *scrib* RNAi clones in the eye already suggested this is not the case. To further examine this idea, we studied both eye and wing disc >>Myc supercompetition to determine whether the competition outcome was altered when WT loser cells were mutant for *fmi*. While the removal of *fmi* caused winner clones to effectively become losers during >>Myc competition (Fig. 2, 3), removing *fmi* from the losers had no effect on the losers' outcome, either in eye discs (Fig. 4A-C) or wing discs (Fig. 4E-F). In both tissues, winner >>Myc clones showed no change in relative size to their twin spot counterparts, nor were loser clones eliminated more effectively (Fig. 4C and 4F).

Our results so far suggested that the effect Fmi exerts on cell competition does not operate through bidirectional intercellular PCP communication. To further consolidate this hypothesis, we examined the effect of removing a dedicated core PCP protein other than Fmi from >>Myc supercompetitors. Generating $vang^{A3}$ >>Myc clones in the wing disc, we observed that the >>Myc clones were unaffected and remained winners (Suppl. Fig. 3). $vang^{A3}$, >>Myc clones were on average 2.2±0.82 times larger than their RFP twins, not significantly different from the 1.7±0.45 fold value for >>Myc clones (Fig. 2F-G) (Suppl. Fig. 3C).

The activity of Fmi in cell competition does not require its cadherin domains

Our results have so far demonstrated that Fmi is required only in winner cells and that its function in cell competition is independent of PCP. Furthermore, our results rule out a role for Fmi homodimers in directly communicating fitness information between prospective winner and loser cells. However, the possibility remained that Fmi might function through trans-homodimerization between prospective winner cells to sustain winner status via a signal, via adhesion, or both. To ask if Fmi fulfills its role by mediating adhesion, we tested whether we could restore winner status to >>Myc clones that lack Fmi by providing a transgenic *fmi* that lacks the 8 cadherin domains of Fmi (*arm-fmi∆Cad*).

Coexpression of *arm-fmiΔCad* in *fmi*^{E59}, >>Myc clones re-established the ability of these clones to outcompete their neighbors, and they again became supercompetitors (Fig. 5). When comparing the ratio of >>Myc clone cell number to twin-spot cell number, the presence of *arm-fmiΔcad* restores competition to a level comparable to >>Myc supercompetitors (1.43±0.48 GFP/RFP cells vs 1.71±0.45 GFP/RFP cells respectively), far above the 0.49±0.29 value for *fmi*^{E59} >>Myc clones compared to twinspots.

Supercompetitor clones mutant for *fmi* consistently show clone fragmentation (Figs. 2E, 3M, 5B). Despite lacking the cadherin repeats, rescued clones not only restored their supercompetitor status, but fully recovered the ability of >>Myc clones to remain cohesive (Fig. 5C). This suggests that the clone fragmentation we observed is unlikely due to the ability of Fmi to contribute to adhesion and more likely caused by a feature of the competition between WT cells and *fmi*$^{-/-}$ >>Myc loser clones that causes their elimination.

Taken together, these results demonstrate that, while Fmi is essential in winner cells to eliminate less fit neighbors, this effect is independent of PCP or other homodimer-mediated signaling, and independent of Fmi-mediated cell adhesion, suggesting instead an as yet uncharacterized function for Fmi.

Discussion

We have identified a requirement for Fmi in winner cells in both tumorigenic and developmental cell competition models. Cells that would otherwise behave as winners instead behave as losers when they lack Fmi. Fmi is notable in that it is required in cell competition in each of four distinct competition scenarios examined: Ras^{v12} *scrib* RNAi tumors, *scrib* RNAi winner clones in larval eye discs, WT cells *vs* *scrib* RNAi loser clones in pupal eyes, and Myc supercompetitor clones in eye and wing discs. Just how universal this requirement is in other cell competition scenarios in *Drosophila* and perhaps in competition in other organisms remains to be determined.

Fmi acts in cell competition independently of PCP

Several arguments support the conclusion that the role for Fmi in cell competition is distinct from its role in PCP signaling. First, Fmi is the only core PCP component among the six that were surveyed to inhibit the ability of Ras^{v12} *scrib* RNAi tumor clones to compete in the eye. If Fmi's role in cell competition were to signal winner fate to losers and vice versa by mirroring its role in PCP signaling, where it signals the presence of proximal (Vang, Pk) components in one direction and the presence of distal components (Fz, Dsh, Dgo) in the other direction between adjacent cells (Lawrence *et al.*, 2004; Strutt and Strutt, 2007; Chen *et al.*, 2008; Strutt and Strutt, 2008; Struhl *et al.*, 2012), then one might expect either the proximal or distal components to also be required in winner clones. No such requirement was observed. Second, in PCP signaling, Fmi functions as a trans-homodimer to transmit those signals and requires the cadherin repeats and other extracellular domains, implying its function as a trans-homodimer (Kimura *et al.*, 2006). In PCP signaling, removing Fmi from either of two adjacent cells completely blocks PCP signaling. In contrast, in cell competition, while Fmi is required in winners, removing Fmi from losers has no effect on competition. Thus, the model of bidirectional signaling via Fmi is not supported by our results.

These observations, however, do not rule out the possibility that Fmi trans-homodimers contribute to intercellular signaling among winner cells. Nonetheless, as discussed above, adhesion seems not to be a meaningful part of the function for Fmi in winners, as an adhesion deficient Fmi construct (*fmiΔCad*) fully rescues both competition and clone adhesion. The potential contributions of adhesion vs other possible signaling mechanisms are discussed at more length below.

Unlike the other core PCP genes, *fmi*$^{-/-}$ mutations are lethal due to requirements in the nervous system (Usui *et al.*, 1999). Though not fully characterized, it's roles in the nervous system appear to be distinct from PCP signaling. Fmi is required for outgrowth and guidance of the R8 axon of the eye to the M3 layer of the medulla via a mechanism that appears independent of other components of the core PCP signaling pathway (Gao *et al.*, 2000; Lee *et al.*, 2003; Senti *et al.*, 2003), but does interact with Golden goal, a transmembrane phosphoprotein that is not associated with PCP signaling (Takechi *et al.*, 2021)**.** Growth of the dendrites of dorsal da neurons is also regulated by Fmi. During embryogenesis, da dendrites in *fmi* mutant embryos emerge precociously and overgrow as they approach the dorsal midline, and later, during larval growth, dendrites from opposite sides fail to avoid each other (tile) and instead overlap (Gao *et al.*, 2000; Sweeney *et al.*, 2002; Kimura *et al.*, 2006)**.**

Fmi is classified as an atypical cadherin and a Class-B adhesion G Protein-Coupled Receptor (aGPCR), as it contains in its extracellular domain several conserved functional domains including cadherin repeats, epidermal growth factor-like repeats, laminin A G-type repeats, a GPCR autoproteolytic inducing (GAIN) domain that contains within it a GPCR proteolytic site (GPS) (Rosa *et al.*, 2021; Einspahr and Tilley, 2022; Sreepada *et al.*, 2022). These extracellular domains are followed by seven transmembrane domains and an intracellular C-terminal domain. Although much remains to be learned about this large subfamily of GPCRs, a general model has emerged in which activation by membrane bound or extracellular protein, peptide, proteoglycan or small molecule ligand, or mechanical force exposes a tethered ligand at the N-terminus of the C-terminal fragment in the GAIN domain that, upon exposure, interacts with the transmembrane portion to activate a G-protein signaling cascade. In many but not all aGPCRs, the tethered ligand is exposed by GAIN domain-mediated autoprotolysis of its GPS. Non-cleaved aGPCRs are hypothesized to expose the tethered ligand by an allosteric conformational change. Some de-orphanized aGPCRs interact with multiple ligands, and ligand binding can result in partial or full activation. In some cases, it appears that engineered truncation of portions of the extracellular domain can produce some level of ligand independent activation (Rosa *et al.*, 2021) .

When expressed in da neurons, a Fmi construct lacking the cadherin, laminin G and EGF-like repeats partially rescued the embryonic dendritic overgrowth phenotype (Kimura *et al.*, 2006), suggesting a function independent of homodimerization. The G protein Gαq (Gq) has been proposed to function downstream of Fmi to mediate this repressive function (Wang *et al.*, 2016). Notably, our results showed that a similar Fmi construct lacking the cadherin domains substantially rescues the requirement for Fmi in winner cells during cell competition (Fig. 5). These observations suggest that supplying adhesion is not the principal function of Fmi in these events, but are consistent with the possibility that homodimeric adhesion, or interaction with a different ligand, normally activates the receptor, and that the truncated FmiΔCad behaves as a constitutively activated receptor. While no biochemical characterization of Fmi has been reported, the human orthologs CELSR1-3 have been studied in detail. CELSR2 is autoproteolytically cleaved while CELSRs 1 and 3 are not, yet all three couple to GαS (Huong Bui *et al.*, 2023). Additional efforts will be required to determine the functional ligand(s) for Fmi and whether it signals similarly. Furthermore, aGPCRs participate in a wide variety of developmental and physiologic

events through diverse effectors(Einspahr and Tilley, 2022; Sreepada *et al.*, 2022) . The pathway by which Fmi participates in cell competition remains to be explored.

Fmi, cell competition and cancer

When the first examples of super-competition were observed in Myc clones and the Hippo pathway (de la Cova *et al.*, 2004; Moreno and Basler, 2004; Harvey and Tapon, 2007), they hinted at the possibility that tumors, which behave like super-competitors, could use similar mechanisms to outcompete WT cells. Understanding tumor competition may open new avenues for early detection and therapy (Baker and Li, 2008; Moreno, 2008).

Research in *Drosophila* and mammals have shown that cell competition plays a dual role during tumorigenesis. Cells harboring mutations in proto-oncogenes or tumor-suppressor genes often behave as losers (Maruyama and Fujita, 2017; Kanda and Igaki, 2020; Morata and Calleja, 2020). Through the process of EDAC, epithelial tissues use cell competition to eliminate transformed pre-neoplastic cells by removing them from the tissue via directed cell death or extrusion(Kon *et al.*, 2017; Watanabe *et al.*, 2018). Pre-neoplastic cells that escape EDAC may accumulate additional mutations to become malignant tumors (Watanabe *et al.*, 2018). Malignant tumors not only escape EDAC, but acquire properties that allow them to outcompete WT cells, facilitating invasion and metastasis (Suijkerbuijk *et al.*, 2016; Kohashi *et al.*, 2021). Furthermore, competition between clones within tumors further selects for more aggressive tumor behavior (Parker *et al.*, 2021).

Another commonality between developmental and oncogenic cell competition is the involvement of the transmembrane protein Flower (Fwe). In both *Drosophila* and mammals, multiple isoforms of Fwe signal fitness; expression of Fwe^{Lose} isoforms mark losers for elimination (Rhiner *et al.*, 2010; Merino *et al.*, 2013; Levayer *et al.*, 2015; Madan *et al.*, 2019). Forced expression of Fwe^{Lose} induces cell competition and elimination of the loser, suggesting that Fwe comparison is involved in the sensing and/or initiation of differential fitness. This contrasts with Fmi, whose differential expression does not act as a trigger for competition, but which is needed in winners to allow them to win, suggesting that Fmi is involved after sensing in the execution of functions necessary to manifest winner behavior.

Evidence is accumulating that a human ortholog of Fmi, CELSR3, is expressed at high levels in a range of solid tumors, including lung, prostate, pancreatic, hepatic, ovarian and colorectal cancers, and in some cases has been shown to be associated with poor prognosis (Katoh and Katoh, 2007; Erkan *et al.*, 2010; Asad *et al.*, 2014; Goryca *et al.*, 2018; Chen *et al.*, 2021a; Li *et al.*, 2021)**.** If CELSR3 is promoting winner cell behavior in these tumors, as might be predicted from its function in *Drosophila*, this could provide the rationale for future efforts to understand the mechanism by which Fmi/CELSR3 facilitates cell competition, with the goal of identifying an intervention that could blunt or perhaps even eliminate the aggressiveness of an array of highly morbid cancers.

Material and methods

Fly stocks and husbandry

Flies were maintained in standard fly food in a temperature-controlled incubator at either 25ºC or 18ºC. Egg collections were performed over a timespan of 24 or 48 hrs. Vials with eggs were kept at 25ºC until heat-shocked for clone generation or dissected.

Heat-shock was performed on late first instar and early second instar larvae, 48 hrs after egg laying (AEL). Vials were kept at 25ºC after heat-shock until larvae were dissected.

The following fly lines were used for the experiments:

- y, w, hsp-Flp act5C-Gal4, UAS-nGFP to generate wing disc clones.
- ey-Flp ; if /SM5^ ; TM2 / ^TM6b to generate eye disc clones and whole tumors.
- Bloomington TRiP UAS-RNAi lines b33623 (*w* control), b26022 (*fmi*), b31311 (*fz*), b31306 (*dsh*), b34354 (*vang*), b32413 (*pk*), b39073 (*scrib*).
- PCP mutant alleles FRT42D, fmi^{E45} / CyO, FRT42D, fmi^{E59} / CyO, FRT2A, fz^{R52} / TM6b, FRT42D, $vang^{A3}$, FRT42D dgo^{380}, FRT42D $pk^{pk\text{-}sple13}$.
- UAS-scrib RNAi ; act5C>CD2>Gal4, UAS-RFP, UAS-Ras^{V12} / TM6b to make whole eye tumors.
- UAS-scrib RNAi FRT42D, tub-Gal^{80} ; act5C>CD2>Gal4, UAS-RFP, UAS-Ras^{V12} / TM6b to generate tumor clones.
- UAS-scrib RNAi, FRT42D, tub-nRFP / FRT42D tub-Gal^{80} to generate scrib RNAi eye disc clones.
- FRT42D fmi^{E59} / FRT42D, tub-nRFP, tub-Gal^{80} to generate wing disc twin spots.
- UAS-dMyc / TM6b for eye and wing disc supercompetitor clones.
- FRT42D fmi^{E59}, arm-fmiΔCad to rescue wing disc clones.

Genotypes of experimental models

Figure 1

(B) ey-Flp ; act5C>CD2>Gal4, UAS-nRFP / TM6b

(C-H) ey-Flp ; UAS-scrib RNAi / UAS-DCR2 ; act5C>CD2>Gal4, UAS-nRFP, UAS-Ras^{V12} / TM6b crossed to the homozygous UAS-RNAi line noted above.

(J) ey-Flp ; FRT42D Gal^{80} / FRT42D ; act5C>CD2>Gal4, UAS-nRFP / TM6b

(K) ey-Flp ; FRT42D tub-Gal^{80} / FRT42D ; act5C>CD2>Gal4, UAS-nRFP UAS-Ras^{V12} / UAS-*scrib* RNAi

(L) ey-Flp ; FRT42D tub-Gal^{80} / FRT42D fmi^{E45} ; act5C>CD2>Gal4, UAS-nRFP UAS-Ras^{V12} / UAS-*scrib* RNAi

(M) ey-Flp ; act5C>CD2>Gal4, UAS-nRFP UAS-Ras^{V12} / UAS-*scrib* RNAi ; fz^{R52} FRT2A / tub-Gal^{80} FRT2A

(N) ey-Flp ; FRT42D tub-Gal^{80} / FRT42D dgo^{380} ; act5C>CD2>Gal4, UAS-nRFP UAS-Ras^{V12} / UAS-*scrib* RNAi

(O) ey-Flp ; FRT42D tub-Gal^{80} / FRT42D $pk^{pk\text{-}sple13}$; act5C>CD2>Gal4, UAS-nRFP UAS-Ras^{V12} / UAS-*scrib* RNAi

(P) ey-Flp ; FRT42D tub-Gal^{80} / FRT42D $vang^{A3}$; act5C>CD2>Gal4, UAS-nRFP UAS-Ras^{V12} / UAS-*scrib* RNAi

Figure 2

(A) ey-Flp ; FRT42D tub-Gal^{80} / FRT42D; act5C>CD2>Gal4 UAS-nRFP / UAS-dMyc

(B) ey-Flp ; FRT42D tub-Gal^{80} / FRT42D fmi^{E59}; act5C>CD2>Gal4 UAS-nRFP / UAS-dMyc

(D) hsp-Flp act5C-Gal4, UAS-nGFP ; FRT42D tub-nRFP tub-Gal^{80} / FRT42D ; UAS-dMyc / TM6b

(E) hsp-Flp act5C-Gal4, UAS-nGFP ; FRT42D tub-nRFP tub-Gal^{80} / FRT42D *fmi*^{E59} ; UAS-dMyc / TM6b

(F) ey-Flp ; FRT42D tub-Gal80 / FRT42D ; act5C>CD2>Gal4 UAS-nRFP / TM6b

(G) ey-Flp ; FRT42D tub-Gal80 / FRT42D ; act5C>CD2>Gal4 UAS-nRFP / UAS-*scrib* RNAi *puc*^{E69}

(H) ey-Flp ; FRT42D tub-Gal80 / FRT42D *fmi*^{E59} ; act5C>CD2>Gal4 UAS-nRFP / UAS-*scrib* RNAi *puc*^{E69}

(I) ey-Flp ; FRT42D *fmi*^{E59} tub-Gal80 / FRT42D ; act5C>CD2>Gal4 UAS-nRFP / UAS-*scrib* RNAi *puc*^{E69}

Figure 3

(A-C) ey-Flp ; UAS-*scrib* RNAi FRT42D tub-Gal^{80} / FRT42D ; act5C>CD2>Gal4, UAS-nRFP UAS-Ras^{V12} / *puc*^{E69}

(E-G) ey-Flp ; UAS-*scrib* RNAi FRT42D tub-Gal^{80} / FRT42D *fmi*^{E59} ; act5C>CD2>Gal4, UAS-nRFP UAS-Ras^{V12} / *puc*^{E69}

(I-K) ey-Flp ; FRT42D tub-Gal^{80} / FRT42D *fmi*^{E59}; act5C>CD2>Gal4 UAS-nRFP / UAS-dMyc

(L) hsp-Flp act5C-Gal4, UAS-nGFP ; FRT42D tub-nRFP tub-Gal^{80} / FRT42D ; UAS-dMyc / TM6b

(M) hsp-Flp act5C-Gal4, UAS-nGFP ; FRT42D tub-nRFP tub-Gal^{80} / FRT42D *fmi*^{E59} ; UAS-dMyc / TM6b

Figure 4

(A) ey-Flp ; FRT42D tub-Gal^{80} / FRT42D tub-nRFP ; act5C>CD2>Gal4 UAS-nGFP / UAS-dMyc

(B) ey-Flp ; FRT42D *fmi*^{E59} tub-Gal^{80} / FRT42D tub-nRFP ; act5C>CD2>Gal4 UAS-nGFP / UAS-dMyc

(D) hsp-Flp act5C-Gal4, UAS-nGFP ; FRT42D tub-nRFP tub-Gal^{80} / FRT42D ; UAS-dMyc / TM6b

(E) hsp-Flp act5C-Gal4, UAS-nGFP ; FRT42D *fmi*^{E59} tub-nRFP tub-Gal^{80} / FRT42D ; UAS-dMyc / TM6b

Figure 5

(A) hsp-Flp act5C-Gal4, UAS-nGFP ; FRT42D tub-nRFP tub-Gal^{80} / FRT42D ; UAS-dMyc / TM6b

(B) hsp-Flp act5C-Gal4, UAS-nGFP ; FRT42D tub-nRFP tub-Gal^{80} / FRT42D *fmi*^{E59} ; UAS-dMyc / TM6b

(C) hsp-Flp act5C-Gal4, UAS-nGFP ; FRT42D tub-nRFP tub-Gal^{80} / FRT42D *fmi*^{E59} arm-*fmiΔCad* ; UAS-dMyc / TM6b

Supplementary Figure 1

(A) ey-Flp ; FRT42D tub-Gal^{80} / FRT42D ; act5C>CD2>Gal4 / UAS-nRFP

(B) ey-Flp ; FRT42D tub-Gal^{80} / FRT42D *fmi*^{E59} ; act5C>CD2>Gal4 / UAS-nRFP

(D-E) hsp-Flp act5C-Gal4, UAS-nGFP ; FRT42D tub-nRFP tub-Gal^{80} / FRT42D *fmi*^{E59} ; MKRS / TM6b

Supplementary figure 2

(A-C) ey-Flp ; FRT42D tub-Gal^{80} / FRT42D *fmi*^{E45} ; act5C>CD2>Gal4, UAS-nRFP UAS-Ras^{V12} / UAS-*scrib* RNAi

Supplementary figure 3

(A-B) hsp-Flp act5C-Gal4, UAS-nGFP ; FRT42D tub-nRFP tub-Gal^{80} / FRT42D *vang*^{A3} ; UAS-dMyc / TM6b

Generation of arm-fmiΔCad

To make the *arm-fmiΔCad* construct, we used cDNA from the *fmi isoform A (stan-RA)* terminally tagged with an HA tag, fused using a SGGGGS linker (*fmi::HA*). We subcloned by Gibson assembly a PCR fragment containing the coding sequence for *fmi::HA* lacking the first 1328 aa, which contain the 8 cadherin domains (fmi$^{\Delta 1\text{-}1328}$) into a pCaSpeR4 vector backbone with the *armadillo* promoter and a Fz 5'UTR. The pCaSpeR4-armP-*fmiΔCad* construct was introduced into flies by P-element integration, and we used a fly line carrying the construct on chromosome arm 2R.

Wing imaginal disc dissection and immunohistochemistry

Third instar wandering larvae (120 hrs AEL) were dissected by transversally cutting the larva in two halves. The posterior half was discarded, and the anterior part was inverted, after which the fat body and digestive tissue (mouth hooks, salivary glands, and gut) were removed. Inverted larvae were fixed in 4% Paraformaldehyde (PFA) in phosphate buffered saline (PBS) + 0.02% Triton X-100 (PBS-T) for 30 min at room temperature (RT). Fixed larvae were then washed three times with PBS-T and then stained.

For antibody staining, larvae were stained with primary antibodies diluted in PBS-T + 3% Normal Donkey Serum (NDS) overnight (o/n) at 4ºC, and then stained with secondary antibodies and DAPI for 1 hr at room temperature. Stained larvae were then washed three times with PBS. Wing discs were carefully removed from the inverted larva and mounted in Vectashield mounting medium (Vector labs).

We used the following primary antibodies: rabbit α-pHis3 (Millipore), 1:100; rabbit α-Dcp1 (Cell Signaling), 1:100, Secondary staining was performed with Thermo Scientific 546-goat α-rabbit, 1:500.

Immunohistochemistry of third instar larval eye discs

Discs dissected from late third instar larvae were fixed for 5–15 min in 4% paraformaldehyde in PBS at 4°C. Fixed eye discs were washed two times in PBS-T. After blocking for 1 hr in 5% Bovine serum Albumin (BSA) in PBS-T at 4°C, discs were incubated with primary antibodies in the blocking solution overnight at 4°C. Incubations with secondary antibodies were done for 90 min at room temperature in PBS-T. Secondary antibody was washed 3 times with PBS-T. Incubations in phalloidin (1:200) and DAPI (1ug/mL), if required, were done in PBS-T for 15 min followed by washing at room temperature before mounting. Stained samples were mounted in 15 µl Vectashield mounting medium (Vector Labs). We used the following primary antibodies: mouse anti-LacZ (1:500 dilution, Promega) rabbit polyclonal anti-cleaved Caspase 3 (1:200 dilution, Abcam). We used the following secondary antibodies from Thermo Scientific: 488-goat α-rabbit, 546-goat α-mouse, 647-donkey α-mouse. Alexa 635 and Alexa 350 conjugated phalloidin.

Image acquisition

Images of whole discs were taken with a Leica SP8 system equipped with a White Light Laser and HyD® detectors. A 40x, NA 1.5 Leica objective and 1.51 refractive index immersion oil were used. Image stacks were taken in 8-bit at 1024x1024 px resolution, and a pinhole of 1 airy unit (AU), using a z-step of 0.3 µM. For automated image quantification pipelines, residual tissue from the leg or haltere discs was

removed in Fiji (fiji.sc, (Schindelin *et al.*, 2012)), as well as the peripodial cells at the apical section of the Z-stack.

Adult eyes and RFP/GFP signal from pupae and eye discs isolated from late third instar larvae were imaged on a Leica MZ16F Stereomicroscope.

Data analysis

Eye imaginal discs representative slices were selected to measure the size of RFP+ clones. To do so, the GFP+ clone area was divided by the non-fluorescent eye disc area to obtain the ratio of GFP+ clone vs non-GFP twin and plotted as the log(ratio) on violin plots including all data points, median and quartiles.

Wing imaginal disc GFP clone and RFP twin spot cell counts were obtained using a set of automated macros written for ImageJ (Bosch and Axelrod, 2023). Cell ratios were obtained as the fraction of GFP+ cells vs RFP+ twin spot cells. Cell ratios were transformed as the log10(ratio) and graphed as violin plots including all datapoints, median and quartiles.

Clone proliferation ratios were measured in ImageJ. First, pHis3 positive cells were located by using the Find maxima function. Then the proliferative ratio of GFP+ cells was obtained by dividing the fraction of pHis3 cells inside GFP clones by the fraction of pHis3 cells outside of GFP+ clones. The proliferative ratio was plotted as a violin plot representing each disc as a data point and indicating the median and quartiles. Statistics used are indicated in the figure legends.

Acknowledgements

We would like to thank members of the Axelrod lab for fruitful discussions. Stocks obtained from the Bloomington Drosophila Stock Center (NIH P40OD018537) were used in this study.

This work was funded by NIH R35GM131914 (J.D.A.) and the Swiss National Science Foundation P400PB_199258 (P.S.B.). The funders had no role in study design, data collection and analysis, decision to publish, or preparation of the manuscript.

Conflict of interest

The authors declare that the research was conducted in the absence of any commercial or financial relationships that could be construed as a potential conflict of interest.

References

Adler PN (2002) Planar signaling and morphogenesis in Drosophila. *Developmental Cell*, **2:** 525–535

Amoyel M, Bach EA (2014) Cell competition: how to eliminate your neighbours. *Development*, **141:** 988–1000

Asad M, Wong MK, Tan TZ, Choolani M, Low J, Mori S, Virshup D, Thiery JP, Huang RY (2014) FZD7 drives in vitro aggressiveness in Stem-A subtype of ovarian cancer via regulation of non-canonical Wnt/PCP pathway. *Cell Death Dis*, **5:** e1346

Baillon L, Germani F, Rockel C, Hilchenbach J, Basler K (2018) Xrp1 is a transcription factor required for cell competition-driven elimination of loser cells. *Sci Rep*, **8:** 17712

Baker NE, Li W (2008) Cell competition and its possible relation to cancer. *Cancer Res*, **68:** 5505–5507

Baker NE (2020) Emerging mechanisms of cell competition. *Nature Reviews Genetics*, **21:** 683–697

Bosch PS, Axelrod JD (2023) Automated counting of Drosophila imaginal disc cell nuclei. *bioRxiv*, 2023.05.26.542420

Brumby AM, Richardson HE (2003) scribble mutants cooperate with oncogenic Ras or Notch to cause neoplastic overgrowth in Drosophila. *EMBO J*, **22:** 5769–5779

Butler MT, Wallingford JB (2017) Planar cell polarity in development and disease. *Nat Rev Mol Cell Biol*, **18:** 375–388

Chen WS, Antic D, Matis M, Logan CY, Povelones M, Anderson GA, Nusse R, Axelrod JD (2008) Asymmetric homotypic interactions of the atypical cadherin flamingo mediate intercellular polarity signaling. *Cell*, **133:** 1093–1105

Chen X, Ma Q, Liu Y, Li H, Liu Z, Zhang Z, Niu Y, Shang Z (2021a) Increased expression of CELSR3 indicates a poor prognostic factor for Prostate Cancer. *J Cancer*, **12:** 1115–1124

Chen Y, Chen Z, Tang Y, Xiao Q (2021b) The involvement of noncanonical Wnt signaling in cancers. *Biomed Pharmacother*, **133:** 110946

Chen ZS, Lin X, Chan TF, Chan HYE (2021c) Pan-cancer investigation reveals mechanistic insights of planar cell polarity gene Fuz in carcinogenesis. *Aging (Albany NY)*, **13:** 7259–7283

Clavería C, Giovinazzo G, Sierra R, Torres M (2013) Myc-driven endogenous cell competition in the early mammalian embryo. *Nature*, **500:** 39–44

Coyle RC, Latimer A, Jessen JR (2008) Membrane-type 1 matrix metalloproteinase regulates cell migration during zebrafish gastrulation: evidence for an interaction with non-canonical Wnt signaling. *Exp Cell Res*, **314:** 2150–2162

de la Cova C, Abril M, Bellosta P, Gallant P, Johnston LA (2004) Drosophila myc regulates organ size by inducing cell competition. *Cell*, **117:** 107–116

de Vreede G, Gerlach SU, Bilder D (2022) Epithelial monitoring through ligand-receptor segregation ensures malignant cell elimination. *Science*, **376:** 297–301

Di Giacomo S, Sollazzo M, Paglia S, Grifoni D (2017) MYC, Cell Competition, and Cell Death in Cancer: The Inseparable Triad. *Genes (Basel)*, **8:** 120

Einspahr JM, Tilley DG (2022) Pathophysiological impact of the adhesion G protein-coupled receptor family. *Am J Physiol Cell Physiol*, **323:** C640–C647

Ellis SJ, Gomez NC, Levorse J, Mertz AF, Ge Y, Fuchs E (2019) Distinct modes of cell competition shape mammalian tissue morphogenesis. *Nature*, **569:** 497–502

Erkan M, Weis N, Pan Z, Schwager C, Samkharadze T, Jiang X, Wirkner U, Giese NA, Ansorge W, Debus J, Huber PE, Friess H, Abdollahi A, Kleeff J (2010) Organ-, inflammation- and cancer specific transcriptional fingerprints of pancreatic and hepatic stellate cells. *Mol Cancer*, **9:** 88

Froldi F, Ziosi M, Garoia F, Pession A, Grzeschik NA, Bellosta P, Strand D, Richardson HE, Pession A, Grifoni D (2010) The lethal giant larvae tumour suppressor mutation requires dMyc oncoprotein to promote clonal malignancy. *BMC Biol*, **8:** 33

Gao FB, Kohwi M, Brenman JE, Jan LY, Jan YN (2000) Control of dendritic field formation in Drosophila: the roles of flamingo and competition between homologous neurons. *Neuron*, **28:** 91–101

Goryca K, Kulecka M, Paziewska A, Dabrowska M, Grzelak M, Skrzypczak M, Ginalski K, Mroz A, Rutkowski A, Paczkowska K, Mikula M, Ostrowski J (2018) Exome scale map of genetic alterations promoting metastasis in colorectal cancer. *BMC Genet*, **19:** 85

Gujral TS, Chan M, Peshkin L, Sorger PK, Kirschner MW, MacBeath G (2014) A noncanonical Frizzled2 pathway regulates epithelial-mesenchymal transition and metastasis. *Cell*, **159:** 844–856

Hariharan IK, Bilder D (2006) Regulation of imaginal disc growth by tumor-suppressor genes in Drosophila. *Annu Rev Genet*, **40:** 335–361

Harvey K, Tapon N (2007) The Salvador-Warts-Hippo pathway - an emerging tumour-suppressor network. *Nat Rev Cancer*, **7:** 182–191

Hogan C, Dupré-Crochet S, Norman M, Kajita M, Zimmermann C, Pelling AE, Piddini E, Baena-López LA, Vincent JP, Itoh Y, Hosoya H, Pichaud F, Fujita Y (2009) Characterization of the interface between normal and transformed epithelial cells. *Nat Cell Biol*, **11:** 460–467

Huong Bui DL, Roach A, Li J, Bandekar SJ, Orput E, Raghavan R, Araç D, Sando R (2023) The adhesion GPCRs CELSR1-3 and LPHN3 engage G proteins via distinct activation mechanisms. *bioRxiv*, 2023.04.02.535287

Ji Z, Chuen J, Kiparaki M, Baker N (2021) Cell competition removes segmental aneuploid cells from Drosophila imaginal disc-derived tissues based on ribosomal protein gene dose. *Elife*, **10:** e61172

Kanda H, Igaki T (2020) Mechanism of tumor-suppressive cell competition in flies. *Cancer Sci*, **111:** 3409–3415

Karim FD, Rubin GM (1998) Ectopic expression of activated Ras1 induces hyperplastic growth and increased cell death in Drosophila imaginal tissues. *Development*, **125:** 1–9

Katoh M (2005) WNT/PCP signaling pathway and human cancer (review). *Oncol Rep*, **14:** 1583–1588

Katoh M, Katoh M (2007) Comparative integromics on non-canonical WNT or planar cell polarity signaling molecules: Transcriptional mechanism of PTK7 in colorectal cancer and that of SEMA6A in undifferentiated ES cells. *International Journal of Molecular Medicine*, **20:** 405–409

Kaucká M, Plevová K, Pavlová S, Janovská P, Mishra A, Verner J, Procházková J, Krejcí P, Kotasková J, Ovesná P, Tichy B, Brychtová Y, Doubek M, Kozubík A, Mayer J, Pospísilová S, Bryja V (2013) The planar cell polarity pathway drives pathogenesis of chronic lymphocytic leukemia by the regulation of B-lymphocyte migration. *Cancer Res*, **73:** 1491–1501

Kimura H, Usui T, Tsubouchi A, Uemura T (2006) Potential dual molecular interaction of the Drosophila 7-pass transmembrane cadherin Flamingo in dendritic morphogenesis. *J Cell Sci*, **119:** 1118–1129

Kohashi K, Mori Y, Narumi R, Kozawa K, Kamasaki T, Ishikawa S, Kajita M, Kobayashi R, Tamori Y, Fujita Y (2021) Sequential oncogenic mutations influence cell competition. *Curr Biol*, **31:** 3984–3995.e5

Kon S, Fujita Y (2021) Cell competition-induced apical elimination of transformed cells, EDAC, orchestrates the cellular homeostasis. *Dev Biol*, **476:** 112–116

Kon S, Ishibashi K, Katoh H, Kitamoto S, Shirai T, Tanaka S, Kajita M, Ishikawa S, Yamauchi H, Yako Y, Kamasaki T, Matsumoto T, Watanabe H, Egami R, Sasaki A, Nishikawa A, Kameda I, Maruyama T, Narumi R, Morita T, Sasaki Y, Enoki R, Honma S, Imamura H, Oshima M, Soga T, Miyazaki JI, Duchen MR, Nam JM, Onodera Y, Yoshioka S, Kikuta J, Ishii M, Imajo M, Nishida E, Fujioka Y, Ohba Y, Sato T, Fujita Y (2017) Cell competition with normal epithelial cells promotes apical extrusion of transformed cells through metabolic changes. *Nat Cell Biol*, **19:** 530–541

Lawrence PA, Casal J, Struhl G (2004) Cell interactions and planar polarity in the abdominal epidermis of Drosophila. *Development*, **131:** 4651–4664

Lee RC, Clandinin TR, Lee CH, Chen PL, Meinertzhagen IA, Zipursky SL (2003) The protocadherin Flamingo is required for axon target selection in the Drosophila visual system. *Nat Neurosci*, **6:** 557–563

Levayer R, Hauert B, Moreno E (2015) Cell mixing induced by myc is required for competitive tissue invasion and destruction. *Nature*, **524:** 476–480

Li Y, Zhu L, Hao R, Li Y, Zhao Q, Li S (2021) Systematic expression analysis of the CELSR family reveals the importance of CELSR3 in human lung adenocarcinoma. *J Cell Mol Med*, **25:** 4349–4362

Madan E, Palma AM, Vudatha V, Trevino JG, Natarajan KN, Winn RA, Won KJ, Graham TA, Drapkin R, McDonald SAC, Fisher PB, Gogna R (2022) Cell Competition in Carcinogenesis. *Cancer Res*, **82:** 4487–4496

Madan E, Pelham CJ, Nagane M, Parker TM, Canas-Marques R, Fazio K, Shaik K, Yuan Y, Henriques V, Galzerano A, Yamashita T, Pinto MAF, Palma AM, Camacho D, Vieira A, Soldini D, Nakshatri H, Post SR, Rhiner C, Yamashita H, Accardi D, Hansen LA, Carvalho C, Beltran AL, Kuppusamy P, Gogna R, Moreno E (2019) Flower isoforms promote competitive growth in cancer. *Nature*, **572:** 260–264

Maruyama T, Fujita Y (2017) Cell competition in mammals - novel homeostatic machinery for embryonic development and cancer prevention. *Curr Opin Cell Biol*, **48:** 106–112

Merino MM, Rhiner C, Lopez-Gay JM, Buechel D, Hauert B, Moreno E (2015) Elimination of unfit cells maintains tissue health and prolongs lifespan. *Cell*, **160:** 461–476

Merino MM, Rhiner C, Portela M, Moreno E (2013) “Fitness fingerprints” mediate physiological culling of unwanted neurons in Drosophila. *Curr Biol*, **23:** 1300–1309

Meyer SN, Amoyel M, Bergantiños C, de la Cova C, Schertel C, Basler K, Johnston LA (2014) An ancient defense system eliminates unfit cells from developing tissues during cell competition. *Science*, **346:** 1258236

Morata G (2021) Cell competition: A historical perspective. *Dev Biol*, **476:** 33–40

Morata G, Calleja M (2020) Cell competition and tumorigenesis in the imaginal discs of Drosophila. *Semin Cancer Biol*, **63:** 19–26

Morata G, Ripoll P (1975) Minutes: mutants of drosophila autonomously affecting cell division rate. *Dev Biol*, **42:** 211–221

Moreno E (2008) Is cell competition relevant to cancer. *Nat Rev Cancer*, **8:** 141–147

Moreno E, Basler K (2004) dMyc transforms cells into super-competitors. *Cell*, **117:** 117–129

Nieto M, Huang R-J, Jackson R, Thiery J (2016) EMT: 2016. *Cell*, **166:** 21–45

Norman M, Wisniewska KA, Lawrenson K, Garcia-Miranda P, Tada M, Kajita M, Mano H, Ishikawa S, Ikegawa M, Shimada T, Fujita Y (2012) Loss of Scribble causes cell competition in mammalian cells. *J Cell Sci*, **125:** 59–66

Ogawa M, Kawarazaki Y, Fujita Y, Naguro I, Ichijo H (2021) FGF21 Induced by the ASK1-p38 Pathway Promotes Mechanical Cell Competition by Attracting Cells. *Curr Biol*, **31:** 1048–1057.e5

Pagliarini RA, Xu T (2003) A genetic screen in Drosophila for metastatic behavior. *Science*, **302:** 1227–1231

Parker TM, Gupta K, Palma AM, Yekelchyk M, Fisher PB, Grossman SR, Won KJ, Madan E, Moreno E, Gogna R (2021) Cell competition in intratumoral and tumor microenvironment interactions. *EMBO J*, **40:** e107271

Pérez E, Lindblad JL, Bergmann A (2017) Tumor-promoting function of apoptotic caspases by an amplification loop involving ROS, macrophages and JNK in Drosophila. *eLife*, **6:**

Puvirajesinghe TM, Bertucci F, Jain A, Scerbo P, Belotti E, Audebert S, Sebbagh M, Lopez M, Brech A, Finetti P, Charafe-Jauffret E, Chaffanet M, Castellano R, Restouin A, Marchetto S, Collette Y, Gonçalvès A, Macara I, Birnbaum D, Kodjabachian L, Johansen T, Borg JP (2016) Identification of p62/SQSTM1 as a component of non-canonical Wnt VANGL2-JNK signalling in breast cancer. *Nat Commun*, **7:** 10318

Rachagani S, Senapati S, Chakraborty S, Ponnusamy MP, Kumar S, Smith LM, Jain M, Batra SK (2011) Activated KrasG^{12}D is associated with invasion and metastasis of pancreatic cancer cells through inhibition of E-cadherin. *Br J Cancer*, **104:** 1038–1048

Rhiner C, López-Gay JM, Soldini D, Casas-Tinto S, Martín FA, Lombardía L, Moreno E (2010) Flower Forms an Extracellular Code that Reveals the Fitness of a Cell to its Neighbors in Drosophila. *Developmental Cell*, **18:** 985–998

Rosa M, Noel T, Harris M, Ladds G (2021) Emerging roles of adhesion G protein-coupled receptors. *Biochem Soc Trans*, **49:** 1695–1709

Schindelin J, Arganda-Carreras I, Frise E, Kaynig V, Longair M, Pietzsch T, Preibisch S, Rueden C, Saalfeld S, Schmid B, Tinevez J-Y, White DJ, Hartenstein V, Eliceiri K, Tomancak P, Cardona A (2012) Fiji: an open-source platform for biological-image analysis. *Nature Methods*, **9:** 676–682

Senti KA, Usui T, Boucke K, Greber U, Uemura T, Dickson BJ (2003) Flamingo regulates R8 axon-axon and axon-target interactions in the Drosophila visual system. *Curr Biol*, **13:** 828–832

Shao DD, Xue W, Krall EB, Bhutkar A, Piccioni F, Wang X, Schinzel AC, Sood S, Rosenbluh J, Kim JW, Zwang Y, Roberts TM, Root DE, Jacks T, Hahn WC (2014) KRAS and YAP1 converge to regulate EMT and tumor survival. *Cell*, **158:** 171–184

Simons M, Mlodzik M (2008) Planar cell polarity signaling: from fly development to human disease. *Annual review of genetics*, **42:** 517–540

Sreepada A, Tiwari M, Pal K (2022) Adhesion G protein-coupled receptor gluing action guides tissue development and disease. *J Mol Med (Berl)*, **100:** 1355–1372

Struhl G, Casal J, Lawrence PA (2012) Dissecting the molecular bridges that mediate the function of Frizzled in planar cell polarity. *Development*, **139:** 3665–3674

Strutt D, Strutt H (2007) Differential activities of the core planar polarity proteins during Drosophila wing patterning. *Dev Biol*, **302:** 181–194

Strutt H, Strutt D (2008) Differential stability of flamingo protein complexes underlies the establishment of planar polarity. *Curr Biol*, **18:** 1555–1564

Suijkerbuijk SJ, Kolahgar G, Kucinski I, Piddini E (2016) Cell Competition Drives the Growth of Intestinal Adenomas in Drosophila. *Curr Biol*, **26:** 428–438

Sweeney NT, Li W, Gao FB (2002) Genetic manipulation of single neurons in vivo reveals specific roles of flamingo in neuronal morphogenesis. *Dev Biol*, **247:** 76–88

Takechi H, Hakeda-Suzuki S, Nitta Y, Ishiwata Y, Iwanaga R, Sato M, Sugie A, Suzuki T (2021) Glial insulin regulates cooperative or antagonistic Golden goal/Flamingo interactions during photoreceptor axon guidance. *Elife*, **10:** e66718

Tsachaki M, Sprecher SG (2012) Genetic and developmental mechanisms underlying the formation of the Drosophila compound eye. *Developmental Dynamics*, **241:** 40–56

Usui T, Shima Y, Shimada Y, Hirano S, Burgess RW, Schwarz TL, Takeichi M, Uemura T (1999) Flamingo, a seven-pass transmembrane cadherin, regulates planar cell polarity under the control of Frizzled. *Cell*, **98:** 585–595

VanderVorst K, Dreyer CA, Hatakeyama J, Bell GRR, Learn JA, Berg AL, Hernandez M, Lee H, Collins SR, Carraway KL (2023) Vangl-dependent Wnt/planar cell polarity signaling mediates collective breast carcinoma motility and distant metastasis. *Breast Cancer Res*, **25:** 52

VanderVorst K, Hatakeyama J, Berg A, Lee H, Carraway KL (2018) Cellular and molecular mechanisms underlying planar cell polarity pathway contributions to cancer malignancy. *Semin Cell Dev Biol*, **81:** 78–87

Vincent JP, Fletcher AG, Baena-Lopez LA (2013) Mechanisms and mechanics of cell competition in epithelia. *Nat Rev Mol Cell Biol*, **14:** 581–591

Vishwakarma M, Piddini E (2020) Outcompeting cancer. *Nat Rev Cancer*, **20:** 187–198

Vladar EK, Antic D, Axelrod JD (2009) Planar cell polarity signaling: the developing cell's compass. *Cold Spring Harb Perspect Biol*, **1:** a002964

Wang Y, Wang H, Li X, Li Y (2016) Epithelial microRNA-9a regulates dendrite growth through Fmi-Gq signaling in Drosophila sensory neurons. *Dev Neurobiol*, **76:** 225–237

Watanabe H, Ishibashi K, Mano H, Kitamoto S, Sato N, Hoshiba K, Kato M, Matsuzawa F, Takeuchi Y, Shirai T, Ishikawa S, Morioka Y, Imagawa T, Sakaguchi K, Yonezawa S, Kon S, Fujita Y (2018) Mutant p53-Expressing Cells Undergo Necroptosis via Cell Competition with the Neighboring Normal Epithelial Cells. *Cell Rep*, **23:** 3721–3729

Weeraratna AT, Jiang Y, Hostetter G, Rosenblatt K, Duray P, Bittner M, Trent JM (2002) Wnt5a signaling directly affects cell motility and invasion of metastatic melanoma. *Cancer Cell*, **1:** 279–288

Wolff T, Ready DF (1991) The beginning of pattern formation in the *Drosophila* compound eye: the morphogenetic furrow and the second mitotic wave. *Development*, **113:** 841–850

Figure 1

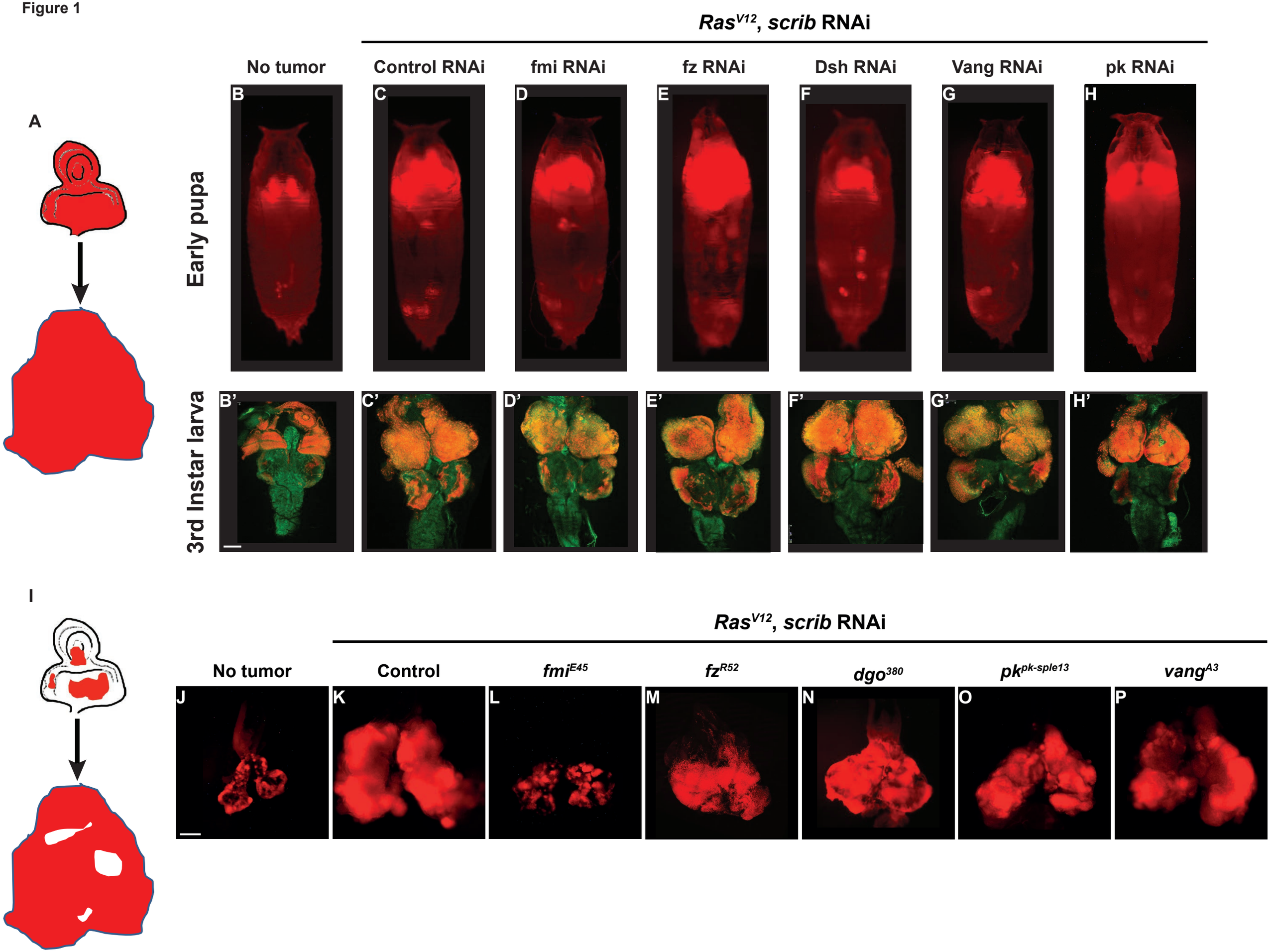
Ras^{V12}, scrib RNAi
No tumor
Control RNAi
fmi RNAi
fz RNAi
Dsh RNAi
Vang RNAi
pk RNAi
A
B
C
D
E
F
G
H
Early pupa
3rd Instar larva
B'
C'
D'
E'
F'
G'
H'
I
Ras^{V12}, scrib RNAi
No tumor
Control
fmi^{E45}
fz^{R52}
dgo^{380}
pk$^{pk\text{-}sple13}$
vang^{A3}
J
K
L
M
N
O
P

Figure 1. Fmi is required in clonal tumors to outcompete WT tissue.

A) Schematic of the whole eye disc Ras^{V12}, scrib RNAi, RFP tumors.

B-H) Pupal RFP tumors imaged through the cuticle. All pupae are ey-Flp ; act5C>CD2>Gal4, UAS-RFP with the indicated RNAi.

C) Control UAS-Ras^{V12}, UAS-scrib RNAi, UAS-w RNAi tumors.

D-H) UAS-RasV12, UAS-scrib RNAi tumors co-expressing UAS-RNAi against the PCP genes indicated above each pupa.

B'-H') Representative third instar larval brain and eye discs for each of the experimental groups from above.

I) Schematic of eye disc Ras^{V12}, scrib RNAi, RFP clonal tumors.

J-P) Third instar larval eye discs RFP tumor clones generated via ey-Flp ; FRT42D Gal80 / FRT42D ; act5C>CD2>Gal4, UAS-RFP.

J) Eye discs with non-tumor, control RFP clones.

K) Control Ras^{V12}, UAS-scrib RNAi, RFP clonal tumors.

L-P) Ras^{V12}, scrib RNAi, RFP clonal tumors carrying the PCP allele indicated above each panel.

Scalebars: 100 µm

Figure 2

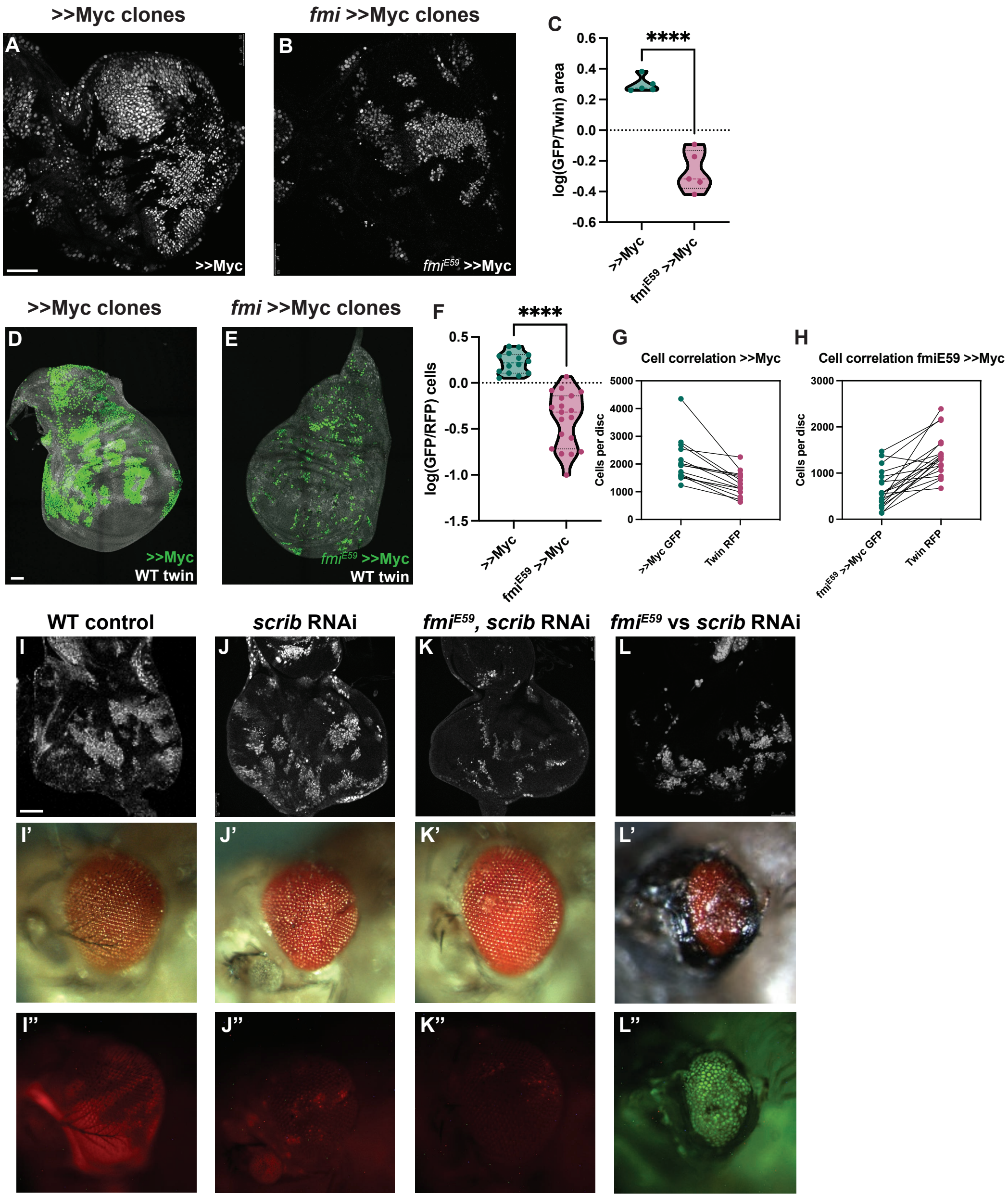
>>Myc clones
fmi >>Myc clones
A
>>Myc
B
fmiE59 >>Myc
C
****
log(GFP/Twin) area
0.6
0.4
0.2
0.0
-0.2
-0.4
-0.6
>>Myc
fmiE59 >>Myc
>>Myc clones
fmi >>Myc clones
D
>>Myc
WT twin
E
fmiE59 >>Myc
WT twin
F
****
log(GFP/RFP) cells
0.5
0.0
-0.5
-1.0
-1.5
>>Myc
fmiE59 >>Myc
G
Cell correlation >>Myc
Cells per disc
5000
4000
3000
2000
1000
0
>>Myc GFP
Twin RFP
H
Cell correlation fmiE59 >>Myc
Cells per disc
3000
2000
1000
0
fmiE59 >>Myc GFP
Twin RFP
WT control
scrib RNAi
fmiE59, scrib RNAi
fmiE59 vs scrib RNAi
I
J
K
L
I'
J'
K'
L'
I''
J''
K''
L''

Figure 2. Winners require Fmi in developmental cell competition.

A) Eye imaginal disc clones overexpressing UAS-Myc (>>Myc) and UAS-nGFP under control of the act5C>CD2>GAL4 driver. Clones were generated with ey-Flp, so half of the cells are clones and the other half are WT twins.

B) Eye imaginal disc >>Myc, UAS-nGFP, *fmi*^{E59} clones, competing against WT twins.

C) Ratio of RFP-labeled clone area versus unlabeled WT area. The unlabeled WT area was obtained by subtracting the RFP-labeled area from the total eye disc area. A ratio over 1 implies RFP-positive clones are supercompetitors, while a ratio below 1 means the RFP-cells are losers. N = 5 discs, groups were analyzed using an unpaired, two-tailed t test; p-value <0.0001 (****)

D) Representative wing imaginal disc overexpressing >>Myc and UAS-nGFP under control of the act5C-Gal4 driver. Clones were generated using hsp70-Flp, with a 15 min 37ºC heat-shock. WT cells are labeled with tub-nRFP. Non-recombinant cells are heterozygous for nRFP, while twin-spots are homozygous nRFP. n = 14 discs

E) Representative wing imaginal disc with >>Myc, UAS-nGFP, *fmi*^{E59} clones, over a WT background. Clones were generated in the same fashion as D. n = 19 discs

F) >>Myc/Twin-spot cell ratio. nGFP total cells were divided by the number of twin-spot homozygous nRFP cells. A ratio over 1 indicates supercompetition of nGFP+ clones, and below 1 indicates nGFP+ cells are losers. The difference between groups was analyzed using an unpaired, two-tailed t test; p-value <0.0001 (****)

G-H) Per-disc assessment of clone size in all >>Myc wing imaginal discs plotted in F. Each dot represents one disc, with the total nGFP cells on the left and total nRFP twin-spot cells on the right.

G) >>Myc clones, behaved as supercompetitors in all discs assayed.

H) >>Myc, *fmi*^{E59} clones, where all but one disc show that the clones are now behaving as losers.

I-L) scrib RNAi clone analysis in the prospective eye. UAS-scrib RNAi was expressed with the act5C>CD2>Gal4 driver and clones were generated by ey-Flp. Clones are marked both with UAS-nGFP and tub-nRFP.

I) Representative disc with control UAS-nGFP clones.

J) UAS-scrib RNAi clones versus WT twin clones.

K) UAS-scrib RNAi, *fmi*^{E59} clones versus WT twin clones.

L) UAS-scrib RNAi clones versus *fmi*^{E59} twin clones. This phenotype was lethal. The adult eye shown in L'/L" was from an escaper. Escapers had trouble eclosing and died within hours.

I'-L') Representative adult eye from the genotypes listed above.

I"-L") Fluorescent expression marking the clones in the adult eyes. In the case of *scrib* RNAi escapers, tub-nRFP fluorescence was barely visible, so the stronger UAS-nGFP is shown.

Scalebars: 50 µm

Figure 3

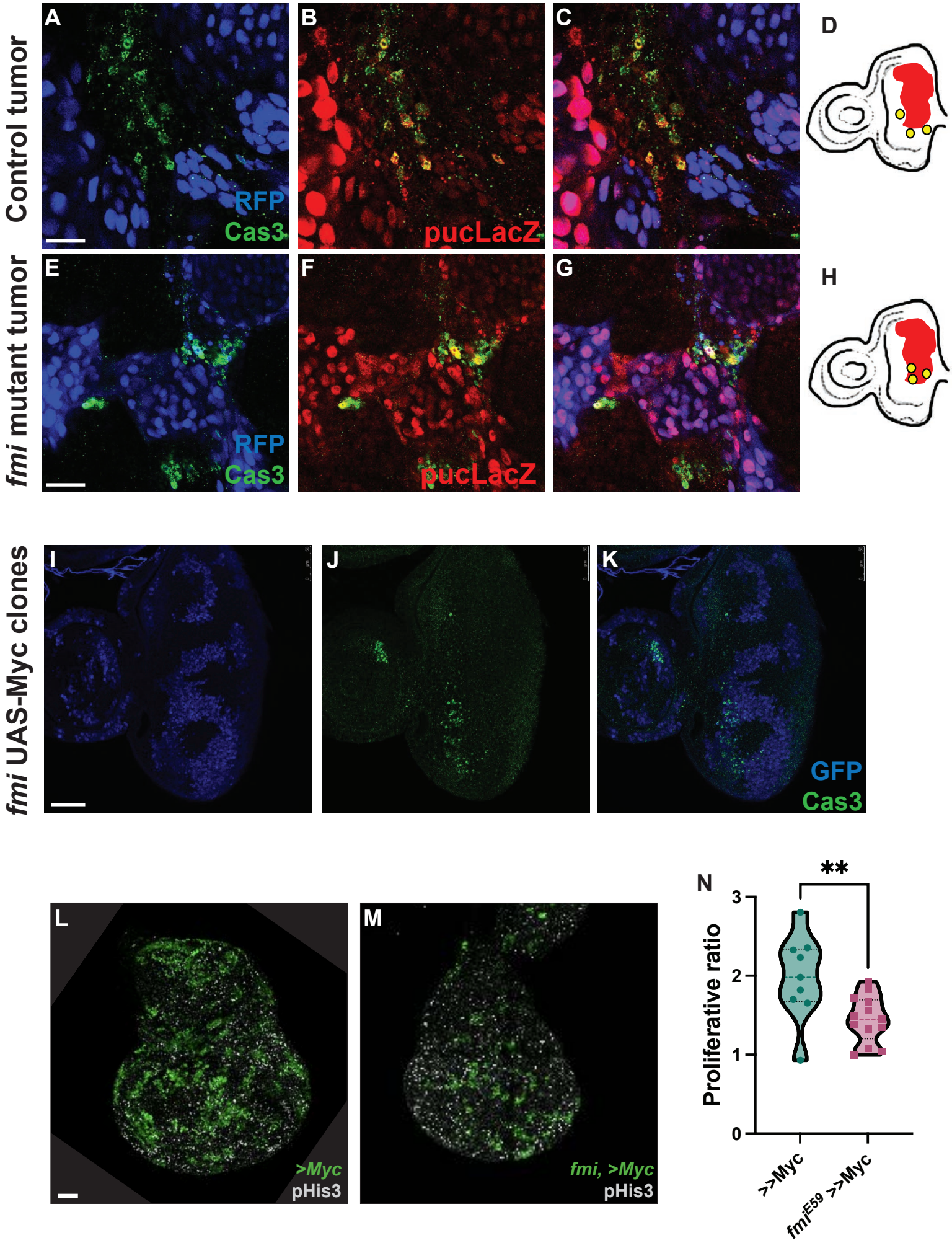
Control tumor
fmi mutant tumor
fmi UAS-Myc clones
A
B
C
D
E
F
G
H
I
J
K
L
M
N
RFP
Cas3
pucLacZ
GFP
>Myc
pHis3
fmi, >Myc
**
Proliferative ratio
0
1
2
3
>>Myc
fmiE59 >>Myc

Figure 3. Lack of Fmi increases cell death and reduces proliferation in would-be winners.

A-C) Ras^{V12}, scrib RNAi tumors stained for DAPI, cleaved Cas3 (A), and puc-lacZ (B). C) Merged channels

D) Representation of how Cas3 staining localizes in the WT cells at the boundary with the tumor.

E-G) Ras^{V12}, scrib RNAi tumors mutant for Fmi, stained with DAPI, cleaved Cas3 (E), and puc-LacZ (F). G) Merged channels.

H) Representation of how Cas3 staining localizes in the tumor cells in contact with the surrounding WT tissue.

Scalebar for A-G: 25 µm

I-K) Cleaved Cas3 staining in >>Myc clones lacking Fmi in the eye disc. Eye disc Myc clones are marked by GFP (I) and were stained for cleaved Cas3 (J). K) Merged channels, showing apoptotic cells localized only in the Myc, fmi^{E59} clones.

Scalebar: 50 µm

L-M) Proliferation analysis performed by pHis3 staining in wing discs with either >>Myc clones (L) or >>Myc, fmi^{E59} clones (M).

Scalebar: 50 µm

N) Proliferative ratio of GFP cells in >>Myc (n=9 discs) versus >>Myc, fmi^{E59} (n=13 discs) clones. The proliferative ratio for each group was calculated as the ratio of pHis3 cells within the GFP+ clone versus the non-GFP WT tissue and the differences were analyzed as an unpaired, two-tailed t test, with a p-value = 0.0073 (**)

Figure 4

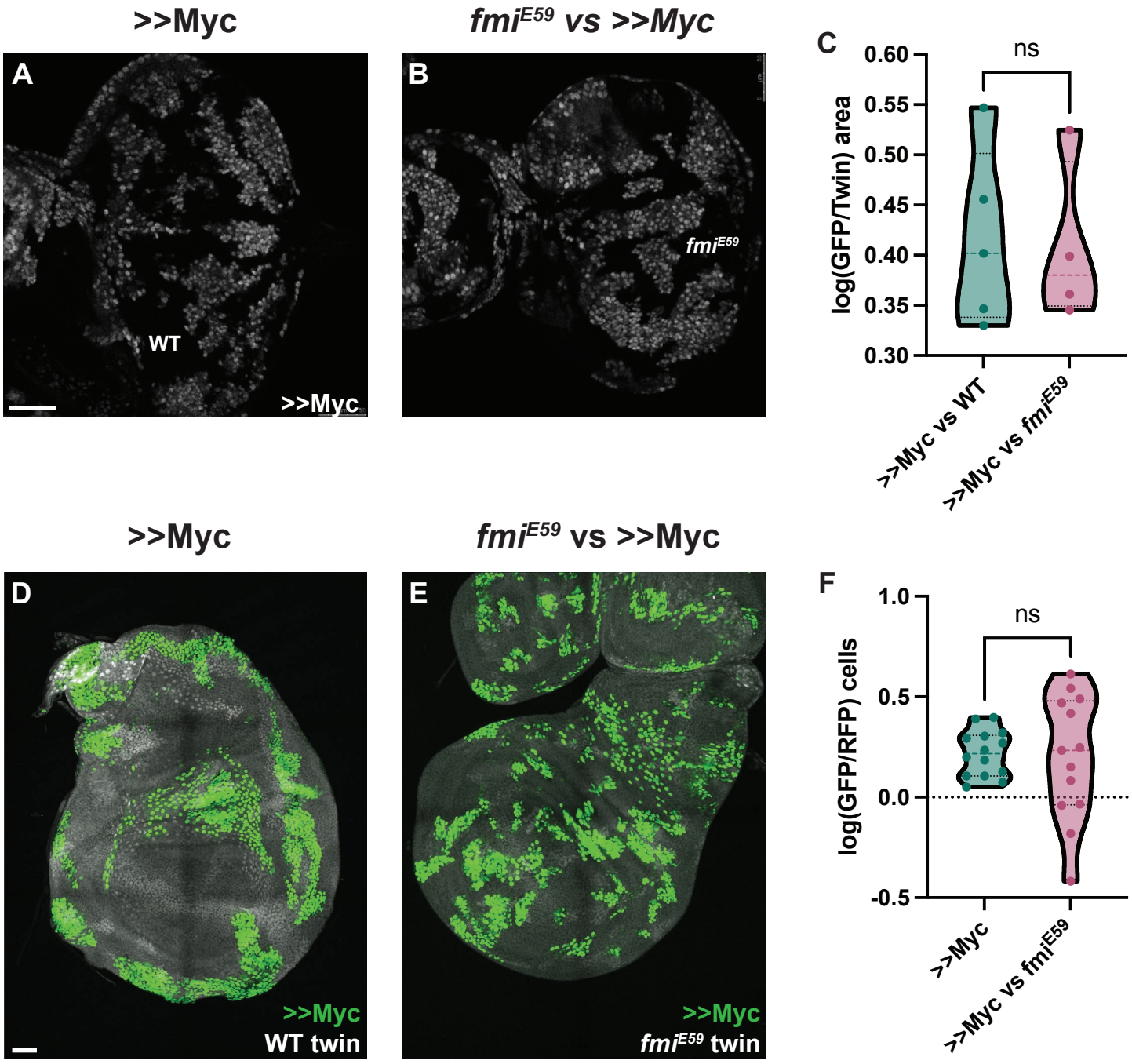
>>Myc
fmiE59 vs >>Myc
A
WT
>>Myc
B
fmiE59
C
ns
log(GFP/Twin) area
0.60
0.55
0.50
0.45
0.40
0.35
0.30
>>Myc vs WT
>>Myc vs fmiE59
>>Myc
fmiE59 vs >>Myc
D
>>Myc
WT twin
E
>>Myc
fmiE59 twin
F
ns
log(GFP/RFP) cells
1.0
0.5
0.0
-0.5
>>Myc
>>Myc vs fmiE59

Figure 4. Eliminating Fmi from the losers does not affect cell competition.

A-B) GFP-labeled, >>Myc supercompetitor clones competing against WT (A) or *fmi*^{E59} (B) cells in the eye imaginal disc. Clones were generated by ey-Flp.

C) Ratio of >>Myc clone vs twin clone area, plotted as the log10(ratio). The differences between WT clones (n=5 discs) versus *fmi*^{E59} (n=4 discs) were analyzed with an unpaired, two-tailed t test, returning a p-value = 0.8837

D-E) GFP-labeled, >>Myc supercompetitor clones competing against WT (D) or or *fmi*^{E59} (E) twin-spot cells in the wing imaginal disc. Twin-spot cells are labeled with homozygous tub-nRFP. Clones were generated with hsp70-Flp.

F) Ratio of >>Myc cells vs twin-spot cells, plotted as the log10(ratio). The ratio of >>Myc GFP competing against homozygous nRFP, *fmi*^{E59} cells (n=13 discs) were directly compared to the ratio of GFP >>Myc cells competing against WT nRFP twin-spot (n=14 discs), which were already quantified for Fig. 2F. The differences between groups were analyzed with an unpaired, two-tailed t test, obtaining a p-value = 0.8210

Scalebars: 50 µm

Figure 5

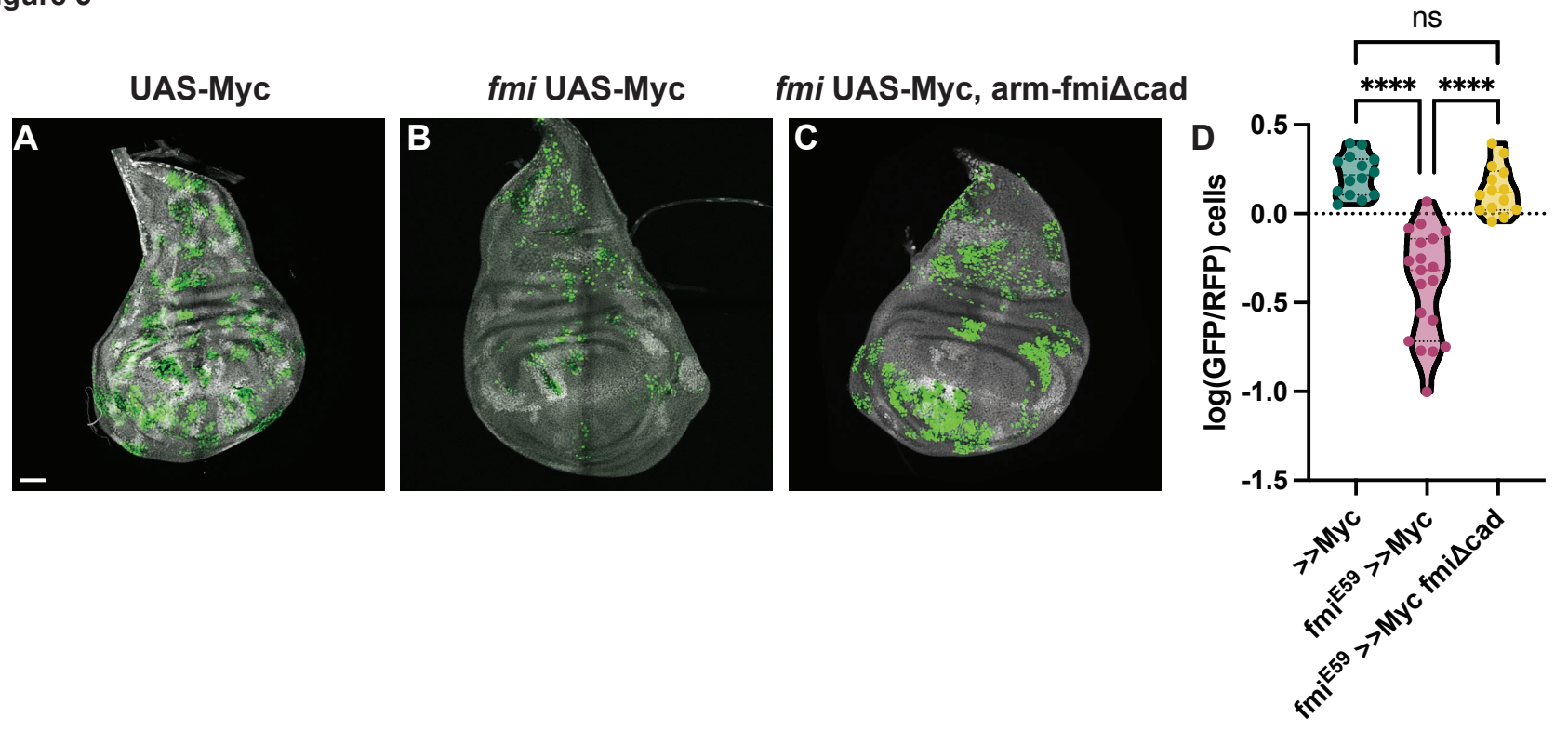
UAS-Myc
fmi UAS-Myc
fmi UAS-Myc, arm-fmiΔcad
A
B
C
D
ns
****
****
0.5
0.0
-0.5
-1.0
-1.5
log(GFP/RFP) cells
>>Myc
fmiE59 >>Myc
fmiE59 >>Myc fmiΔcad

Figure 5. The Fmi cadherin repeats are not required for cell competition.

A) Representative disc with nGFP-labeled, >>Myc (A), >>Myc, *fmi*^{E59} (B) or >>Myc, *fmi*^{E59}, *arm-fmiΔcad* (C) clones competing against WT twin-spots in the wing disc. Twin-spot clones are labeled with homozygous nRFP and clones were generated with hsp70-Flp.

D) Ratio of GFP versus RFP cells in the three groups, represented as the log10(GFP/RFP) cell ratios. To evaluate the effect of the arm-fmiΔcad rescue (n=14 discs), the GFP/RFP cell ratio was directly compared against the two other groups, already quantified and shown in Fig. 2F. Differences between the groups were analyzed using an unpaired, ordinary one-way ANOVA, which found a p-value <0.0001. Inter-group differences were analyzed with a Tukey multiple comparisons test, which found no differences between >>Myc and >>Myc, *fmi*^{E59}, *arm-fmiΔcad* clones, whereas both groups strongly differed from >>Myc, *fmi*^{E59} clones, both returning a p-value <0.0001 (****) when compared directly against >>Myc, *fmi*^{E59}.

Scalebar: 50 µm

Supplementary figure 1

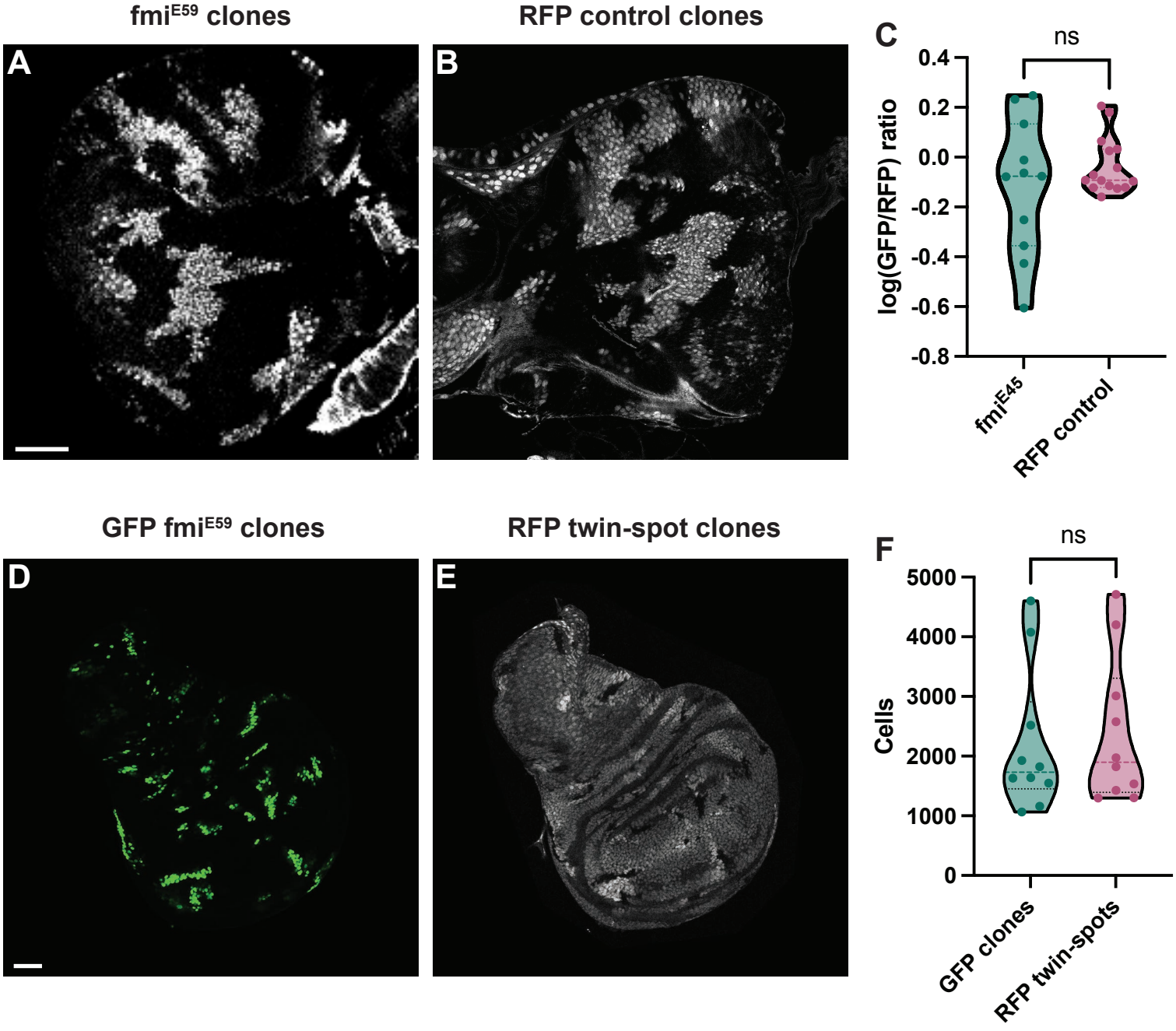

Supplementary figure 1. Fmi by itself does not trigger cell competition

A) Eye disc GFP+ *fmi*^{E59} versus an unlabeled WT background. Clones were generated with ey-Flp as in Fig. 2A.

B) Eye disc GFP+, RFP control clones versus a WT background.

C) log of the GFP/WT clone ratio measured in either *fmi*^{E59} clones vs WT (n=11 discs) or RFP+ clones vs WT (n=15 discs). Differences were analyzed by a two-tailed, unpaired t test, rendering a p-value of 0.7655

D) Representative wing imaginal disc showing the GFP+ *fmi*^{E59} clone cells. Clones were generated with hsp70-Flp.

E) Twin spot RFP+ cells for the disc shown in D. Homozygous RFP+ twin-spots can be observed adjacent to the RFP- *fmi*^{E59} clones.

F) *fmi*^{E59}, GFP cells versus WT RFP twin-spot cells counted in wing imaginal discs (n=10 discs). The differences were analyzed with a two-tailed, ratio-paired t test, p-value = 0.4815

Scalebar: 50 µm

Supplementary figure 2

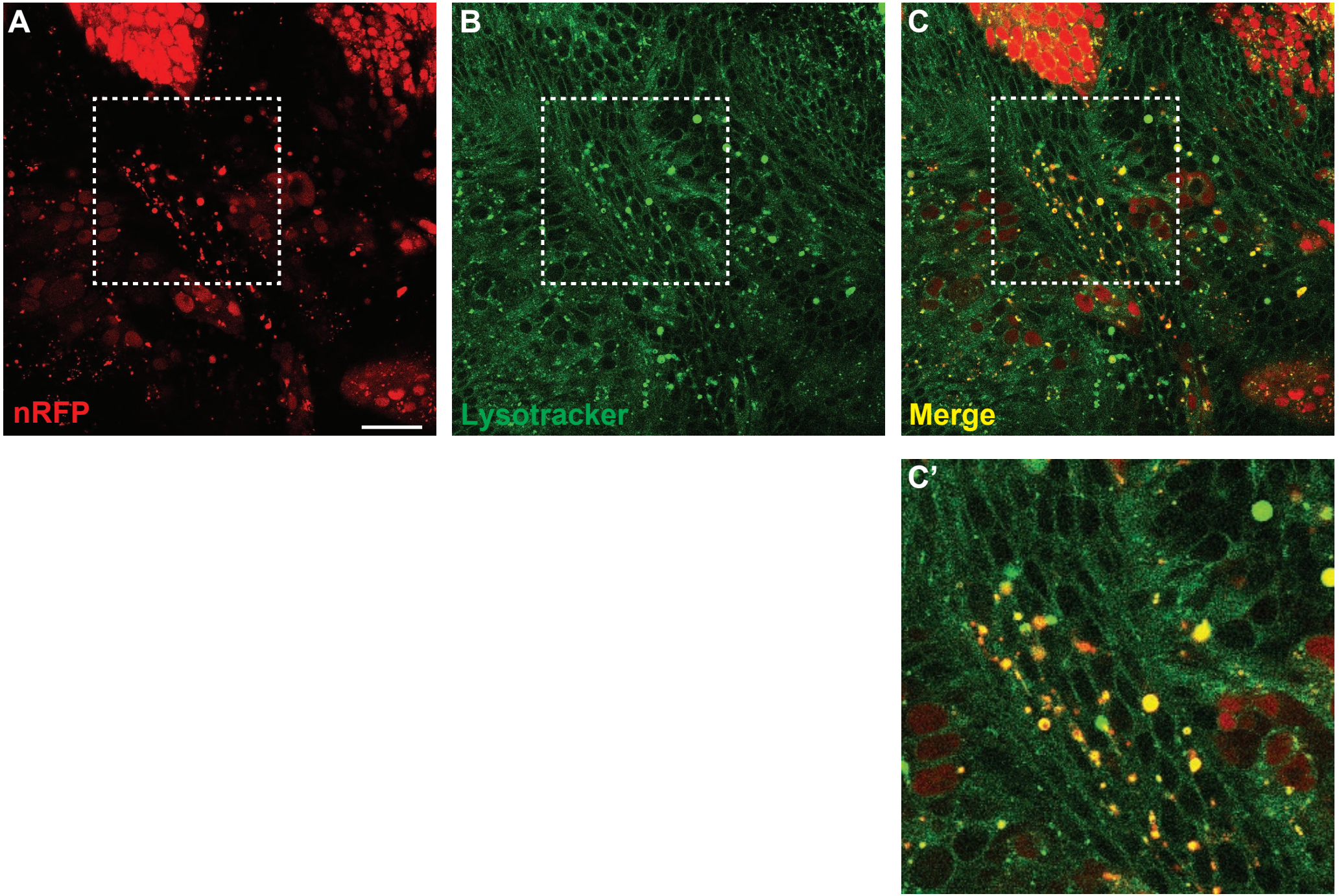

Supplementary figure 2. Fmi-/- tumor cell debris is found in vesicles inside WT cells

A) Close-up of RFP-tagged *fmi*^{E59} RasV12, scrib RNAi tumors competing against unlabeled WT cells in eye discs. RFP+ tumor cells can be observed at the periphery, and RFP+ debris is detected in the unlabeled WT cells inside the annotated area.

B) Lysotracker staining marking acidic vesicles. Large, stained vesicles can be observed in the annotated area.

C) The merged channels show colocalization of the RFP+ cell debris with the lysosomal vesicles inside WT cells.

D) Closeup of the annotated region in panels A-C.

Scale bar: 25 µm

Supplementary Figure 3

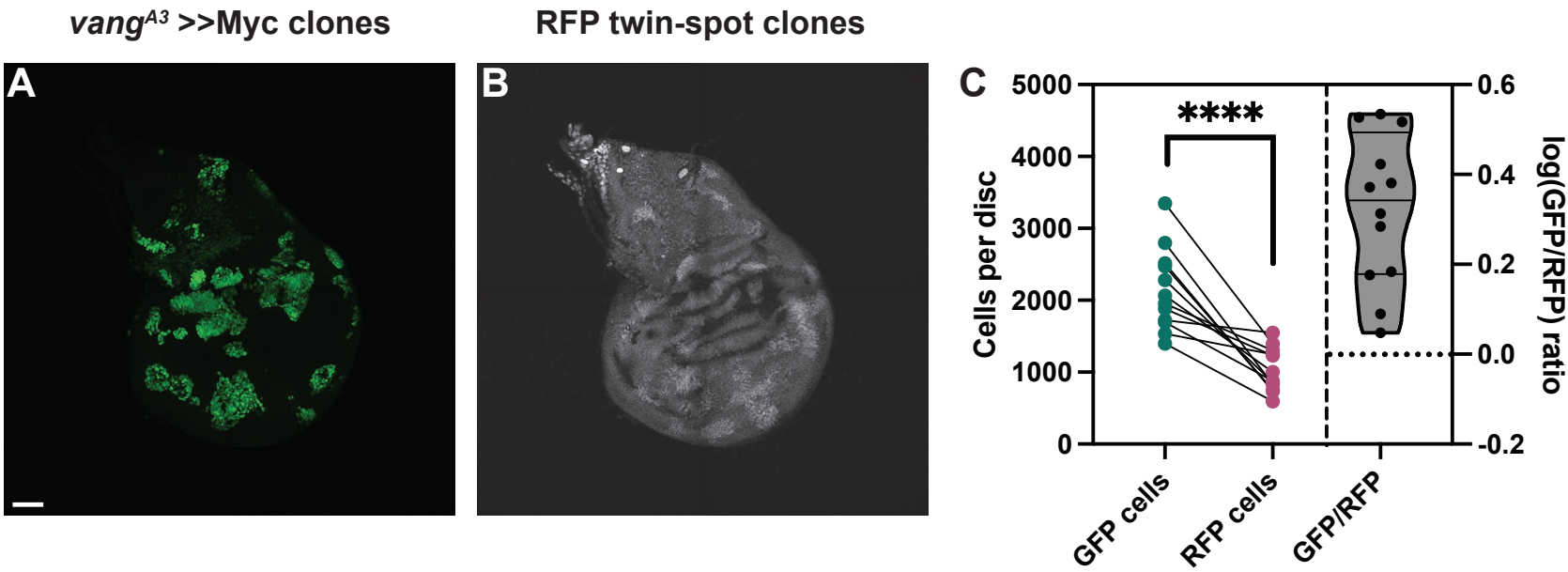

Supplementary figure 3. Vang is not required for >>Myc supercompetition

A) Representative wing imaginal disc showing the GFP-tagged, *vang*^{A3} >>Myc clones. Clones were generated using hsp70-Flp

B) RFP-labeled twin-spots for the clones shown in A. Twin-spot homozygous for RFP can be observed adjacent to the supercompetitor clones.

C) Graph showing the total GFP and RFP counts per disc, with each disc counts linked by a line and the log10 ratio of GFP/RFP cells per disc (n=12 discs). Differences between GFP/RFP clone size were analyzed using a two-tailed, ratio-paired t test. p-value<0.0001. When the ratio was compared with a two-tailed t test to >>Myc, the difference was not significant, with a p-value of 0.078.

Scalebar: 50 µm